

OLFACTORY-IMMUNO PATHWAY OF INFECTIOUS HEMATOPOIETIC
NECROSIS VIRUS AND *YERSINIA RUCKERI* IN RAINBOW TROUT

by

Fabiola Mancha, B.S.

A thesis submitted to the Graduate Council of
Texas State University in partial fulfillment
of the requirements for the degree of
Master of Science
with a Major in Aquatic Resources
August 2021

Committee Members:

Mar Huertas, Chair

Dana M. García

Kelly Woytek

COPYRIGHT

by

Fabiola Mancha

2021

FAIR USE AND AUTHOR'S PERMISSION STATEMENT

Fair Use

This work is protected by the Copyright Laws of the United States (Public Law 94-553, section 107). Consistent with fair use as defined in the Copyright Laws, brief quotations from this material are allowed with proper acknowledgement. Use of this material for financial gain without the author's express written permission is not allowed.

Duplication Permission

As the copyright holder of this work I, Fabiola Mancha, authorize duplication of this work, in whole or in part, for educational or scholarly purposes only.

ACKNOWLEDGEMENTS

First and foremost, I'd like to thank Dr. Mar Huertas for her patience, guidance and encouragement throughout this experience. Her love and passion for science, teaching, and uplifting Hispanic women in STEM is inspiring, and I am forever appreciative for everything I have learned during my time in her lab. Thank you, Dr. Huertas, so much for challenging me and helping me evolve as a writer and scientist. I would also like to thank my committee, Dr. Dana García, and Dr. Kelly Woytek, for taking their time to help me with this project and for introducing and nurturing my love of neurobiology and immunology.

Thanks to all the current and past members of Dr. Huertas lab who were there with me during this journey. Thank you, Dr. Laura Ellis, for your help, support, and patience, both in lab and with writing. I would like to especially thank Melody Martinez and Whitney Ortiz for their constant encouragement, words of positivity, and emotional support. Thank you for your friendship, humor, and constant reassurance during this amazing experience.

Most importantly, I would like to thank my parents, siblings, and grandmother for their unconditional love and patience. Thank you for believing in me and encouraging me to pursue my dreams. You are my biggest supporters and the reason I push forward; everything I do is to make you proud and so that one day I can give back to my community.

TABLE OF CONTENTS

	Page
ACKNOWLEDGEMENTS	iv
LIST OF TABLES	vii
LIST OF FIGURES	viii
LIST OF ABBREVIATIONS	ix
ABSTRACT.....	x
CHAPTER	
1. INTRODUCTION	1
1.1 Fish Olfactory System.....	2
1.2 Integration of Olfactory Responses in the Brain.....	7
1.3 The Role of Neurosteroids in Mediating Inflammatory and Behavioral Responses.....	10
1.4 Infectious Hematopoietic Necrosis Virus and <i>Yersinia ruckeri</i> in Aquaculture.....	13
2. THESIS GOAL	15
3. OBJECTIVES	17
3.1 Tracing OSNs from the Olfactory Rosette to the Brain in Rainbow Trout	17
3.2 Quantifying Neurosteroids in the Olfactory Organ and CNS of Rainbow Trout after Nasal Exposure to Inactivate Pathogens.....	17
3.3 Behavioral Assessment of Rainbow Trout to <i>Y. ruckeri</i>	17
4. MATERIAL AND METHODS	18
4.1 Fish.....	18
4.2 IHNV Vaccine	18
4.3 <i>Y. ruckeri</i> Vaccine.....	18
4.4 Chemical Solutions	19

4.5 Nasal Exposure of Inactivated IHNV and <i>Y. ruckeri</i> for Histology and Neurosteroid Extractions	19
4.6 Tissue Collection and Histology	20
4.7 Steroid Extractions.....	21
4.8 Enzyme-Linked Immunosorbent Assay (ELISA)	22
4.9 Behavior	23
5. RESULTS	26
5.1 Histology: IHNV and <i>Y. ruckeri</i> Neurocircuit Tracing	26
5.2 Biochemical Analysis of Neurosteroids.....	32
5.3 Behavior.....	36
6. DISCUSSION.....	39
7. CONCLUSION.....	51
REFERENCES	52

LIST OF TABLES

Table	Page
1. Summary of Alexa Fluor-Dextran Properties	19
2. Summary of Neurotracing Parameters Utilized for Histology	26

LIST OF FIGURES

Figure	Page
1. Microscopic and Gross Anatomy of Rainbow Trout (<i>Oncorhynchus mykiss</i>) Brain and Olfactory Epithelium.....	6
2. Summary of Steroidogenic Pathways	12
3. Two-Choice Maze for Behavioral Analysis of Rainbow Trout.....	25
4. Fluorescent Micrograph of Olfactory Epithelium Exposed to IHNV and Media.....	27
5. Activated Olfactory Sensory Neurons following Intranasal Delivery of <i>Y. ruckeri</i>	28
6. Olfactory Response to PBS and Water-based <i>Y. ruckeri</i> vaccine	29
7. <i>Y. ruckeri</i> Activates Crypt-like Cells in the Olfactory Epithelium	31
8. Intranasal Delivery of <i>Y. ruckeri</i> Traced to Higher Regions of the Brain	32
9. Olfactory Detection of IHNV Modulates Neurosteroid Concentration in the Olfactory Bulb and Brain.....	33
10. Characterizing the Presence of Neurosteroids in Olfactory Epithelia after Intranasal Delivery of <i>Y. ruckeri</i>	35
11. Olfactory Detection of <i>Y. ruckeri</i> Mediates Neurosteroid Concentrations in the Olfactory Bulb	36
12. Neurosteroid Concentrations in the Rest of Brain Are Modulated after Olfactory Detection of <i>Y. ruckeri</i>	36
13. Two-Choice Maze Behavioral Responses to Food, <i>Y. ruckeri</i> , and Formaldehyde	38

LIST OF ABBREVIATIONS

Abbreviation	Description
AD	Androstenedione
DHEA	Dehydroepiandrosterone
E1	Estrone
E2	Estradiol
F	Cortisol
F-S	Sulphated cortisol
IHNV	Infectious Hematopoietic Necrosis Virus
OB	Olfactory bulb
OE	Olfactory epithelium
OSN	Olfactory sensory neurons
OT	Optic tectum
P-S	Sulphated progesterone
T	Testosterone
<i>Y. ruckeri</i>	<i>Yersinia ruckeri</i>

ABSTRACT

Aquatic pathogens, such as Infectious Hematopoietic Necrosis Virus (IHNV) and *Yersinia ruckeri*, contribute to disease in commercial and wild farms worldwide. These pathogens are highly contagious and frequently cause disease in rainbow trout by infecting them through external tissues, like the gills or skin. Another external tissue, the olfactory organ, is highly susceptible to infection due to the direct contact with the microbe-rich environment. Although the olfactory organ is primarily responsible for detecting environment stimuli, novel research has implicated that olfactory sensory cells also play a key role in early pathogen detection and immune cell activation. Specifically, research has elucidated that IHNV can utilize the olfactory organ as route of entry. However, it is unclear if bacteria act similarly, and we currently lack information regarding the higher levels of integration within the nervous system of rainbow trout. The purpose of this study is to unravel the olfactory pathway involved in the detection of pathogens and the activation of physiological and behavioral response.

1. INTRODUCTION

Neural circuits are pathways comprised of interconnecting cells that carry out a particular function when activated (Lerner, Ye, & Deisseroth, 2016). These pathways generate neural outputs from one cell to the next when chemical substances interact with their specific receptors. Chemical substances involved in modulating neural circuits include neurotransmitters, neuropeptides, and neurosteroids; all of which act by modulating excitatory postsynaptic potentials (EPSP) or inhibitory postsynaptic potentials (IPSP) (Lerner et al., 2016).

Neural circuits in the sensory system are activated by sensory stimuli, internal or external, which then modulate changes within the brain and induce physiological and/or behavioral changes in an organism. For example, an internal change, such as hypoventilation, causes hypercapnia and respiratory acidosis. This, in turn, activates chemoreceptors in respiratory neural circuits (Sunshine, Sutor, Fox, & Fuller, 2020). Likewise, an external noxious stimulus, such as a bite or scratch, activates nociceptors which mediate neural circuits involved in pain (Peirs & Seal, 2016). Other external stimuli include tactile detection of changes in temperature, which activate thermoregulation circuits, visual cues, which activate retinal circuits, or environmental odorants, which activate olfactory circuits through a physiological process known as olfaction (Demb & Singer, 2015).

Olfaction enables organisms to communicate and to navigate their environment through odorant detection. This process specializes in discriminating an array of diverse odorants with high sensitivity and occurs when odorants interact with olfactory receptor proteins found on the apical region of the olfactory sensory neurons (OSNs) (Buck, 1996;

Hamdani & Døving, 2007). Odorant discrimination is vital and facilitates several physiological processes, including reproduction, predator avoidance, prey detection, recognition of conspecifics, and other behavioral processes (Hoover, 2010). However, novel research has also shown that olfaction can mediate the nasal neural immune response (Sepahi et al., 2019)

1.1 Fish Olfactory System

The olfactory system in fish is comprised of external openings and an internal tissue (Hamdani & Døving, 2007; Kasumyan, 2004). The external openings include two pairs of nares, anterior and posterior, situated on the dorsal medial surface of the head (Fig. 1A) (Hamdani & Døving, 2007; Kasumyan, 2004). This arrangement is optimal for odorant detection. Water enters, passively or actively, through the anterior nares and stimulates the internal tissue, before exiting through the posterior nares (Kasumyan, 2004). The olfactory epithelium is an internal tissue that projects from the nasal cavity floor. This tissue is often arranged in a rose-like fashion and is comprised of a series of folds, called lamellae, that converge to the central median raphe (Bazáes & Schmachtenberg, 2012) (Fig. 1C).

The olfactory epithelium is comprised of non-sensory and sensory cells that are arranged in a pseudostratified fashion (Hamdani & Døving, 2007; Kasumyan, 2004) (Fig. 1B). Non-sensory cells include goblet, basal, and supporting cells (also called sustentacular cells) (Hamdani & Døving, 2007; Kasumyan, 2004). Goblet cells secrete mucus, a viscous glycoprotein mixture, that forms a thin layer over the epithelium (Kasumyan, 2004). It is speculated that the mucosal layer creates optimal conditions for the interaction between the odorant and receptor (Kasumyan, 2004). The mucosal layer

also provides a layer of defense against pathogens and prevents mechanical abrasion of the epithelium as water is filtered through the lamellae (Hamdani & Døving, 2007). Basal cells, located at the basal surface of the epithelium, are involved in regeneration, and are thought to be precursors of receptor and supporting cells. Supporting cells help maintain and support the integrity of the olfactory epithelium by enveloping olfactory sensory neurons, but little else of their function is known (Kasumyan, 2004). Supporting cells are also found in mammals and act as a portal of entry for the novel SARS-COV2 virus (severe acute respiratory syndrome coronavirus 2), which may pass directly to cerebrospinal fluid and has been shown to infect the brain in mice (Butowt & Bilinska, 2020).

The sensory region of the olfactory lamellae is comprised of four morphologically distinct olfactory sensory neurons (OSNs); ciliated, microvillus, kappe, and crypt cells (Fig. 1B) (Hansen & Zielinski, 2005; Hansson, Doving, & Skjeldal, 2015). OSNs are bipolar neurons with two extensions: a dendritic extension that projects from the apical surface of the cell and an axonal extension at the basal surface of the cell, that transduces odorants to the olfactory bulb (OB) on the ventral aspect of the brain (Olivares & Schmachtenberg, 2019). The cell body of the various OSNs are situated at different depths in the olfactory epithelium and vary in numbers. Ciliated, microvilli, and crypt cells respectively represent about 90%, 8%, and 2% of the OSNs (Kermen, Franco, Wyatt, & Yaksi, 2013). Kappe neurons are sparse with only a few hundred cells per olfactory organ (Ahuja et al., 2014). The number of total neurons varies between species, number of lamellae and age (Kasumyan, 2004).

The bulk of the epithelium is composed of ciliated olfactory sensory neurons

(cOSNs) (Hamdani & Døving, 2007). The cell bodies of the cOSNs are situated in the deepest layer and possess long dendrites with 3-10 cilia that extend toward the olfactory pit lumen (Hamdani & Døving, 2007; Kermen et al., 2013). Comparatively, microvillus sensory neurons (mOSNs) possess shorter dendrites, and their cell bodies are located at intermediate depths (Hamdani & Døving, 2007). The apical surface of mOSNs is lined with 30-80 microvilli (Bazaes, Olivares, & Schmachtenberg, 2013; Kasumyan, 2004). These sensory neurons express different types of odorant receptors that respond to different classes of stimuli (Hansson et al., 2015). Both ciliated and microvilli cells in catfish, zebrafish, and rainbow trout are known to respond to amino acids, which indicate the presence of food (Kermen et al., 2013; Miklavc & Valentinčič, 2012; Sato & Suzuki, 2001).

Although ciliated and microvilli cells are present in higher vertebrates, crypt and kappe OSNs are exclusive to fish (Ahuja et al., 2014; Biechl, Tietje, Gerlach, & Wullimann, 2016; Gerlach et al., 2019). Both crypt and kappe cells are apically positioned but are distinguishable by their globular and pear-shaped morphology, respectively (Fig 1D; (Ahuja et al., 2014; Biechl et al., 2016). Crypt cells contain short cilia and microvilli projecting from the apical surface, while studies suggest that kappe cells only possess microvilli (Ahuja et al., 2014; Biechl et al., 2016). The exact roles of crypt and kappe cells remains elusive. Current studies have implicated crypt cells in the detection of amino acids, bile acids, or reproductive pheromones in juvenile trout (Kermen et al., 2013; Vielma, Ardiles, Delgado, & Schmachtenberg, 2008). Crypt cells have also been shown to be involved in kin recognition in larval zebrafish and in mediating antiviral immune responses in rainbow trout (Biechl et al., 2016; Sepahi et al.,

2019). However, much less is known of the role of kappe cells, a newly identified population of OSNs (Ahuja et al., 2014). All OSNs transmit olfactory information through a cascade of signaling pathways that is relayed to the central nervous system (CNS) (Antunes, Sebastião, & Simoes de Souza, 2014).

Each OSN expresses several copies of a single G-protein coupled receptor (GPCR) that responds to odorants in the environment (Bazaes et al., 2013; Buck, 1996). This interaction starts the transduction process, which results in a change in the membrane potential that culminates in the generation of an action potential in the axon of olfactory sensory neurons (Buck, 1996; Wetzel, Brunert, & Hatt, 2005). Axonal projections of olfactory sensory neurons expressing the same receptor then converge onto specific glomeruli in the olfactory bulb (Buck, 1996; Miklavc & Valentinčič, 2012; Sato & Suzuki, 2001).

The olfactory bulb receives a large majority of the axonal projections from the olfactory epithelium (Kermen et al., 2013). These axons travel through four regions of the OB; the olfactory nerve layer, glomerular layer, mitral cell layer and granular layer (Olivares & Schmachtenberg, 2019). The outermost most layer of the olfactory bulb, the olfactory nerve layer, contains the axons of OSNs (Kermen et al., 2013; Olivares & Schmachtenberg, 2019). The axons project to spherical structures called glomeruli, although in fish these glomeruli are not as visible as in mammals. These structures contain the dendrites of mitral cells, the cell body of which is found in the mitral cell layer (Kermen et al., 2013; Olivares & Schmachtenberg, 2019). Mitral cells serve two purposes: (1) they act as second order neurons and relay information to higher regions of the CNS and (2) they are modulated by granular cells, which are located in the innermost

layer of the olfactory bulb (Kermen et al., 2013; Olivares & Schmachtenberg, 2019). However, there are some olfactory fibers that traverse the OB to higher regions of the brain (Kermen et al., 2013). In trout, these fibers traverse and innervate the ventral and dorsal telencephalon, preoptic area, and the hypothalamus (Becerra, Manso, Rodriguez-Moldes, & Anadón, 1994).

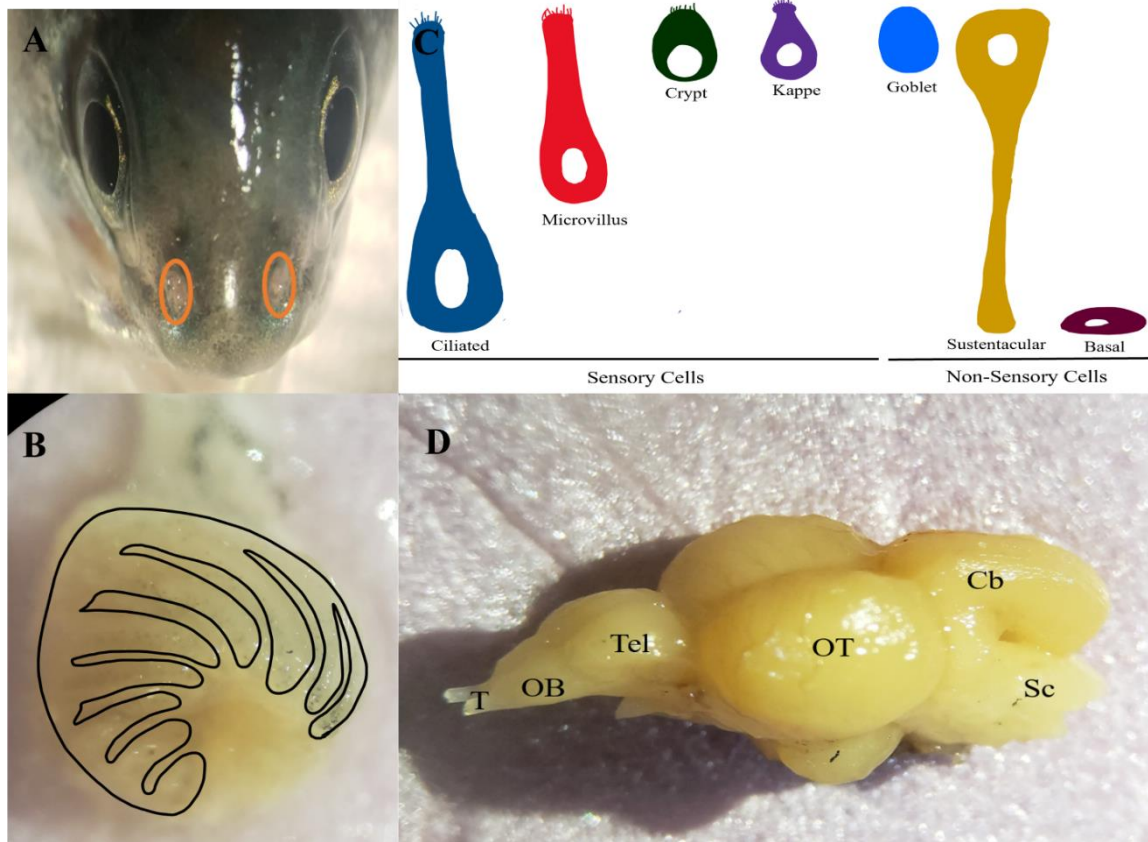


Figure 1. Microscopic and Gross Anatomy of Rainbow Trout (*Oncorhynchus mykiss*) Brain and Olfactory Epithelium. (A) Gross view of nares, indicated by orange circles. (B) Isolated olfactory rosette. (C) Sensory and non-sensory cells of the olfactory epithelium. The cell body of sensory cells are situated at varying depths and include ciliated olfactory sensory neurons (OSNs), microvillus OSNs, crypt OSNs and kappe OSNs. Non-sensory cells include goblet, sustentacular (also known as supporting) and basal cells. (D) Regions of trout brain; Olfactory tract (T), Olfactory bulb (OB), Telencephalon (Tel), Optic Tectum (OT), Cerebellum (Cb), Spinal cord (Sc).

1.2 Integration of Olfactory Responses in the Brain

Direct transmission of odorant electrical signals to the CNS via the olfactory neurons is an immediate process that triggers various physiological processes. However, this route makes the aquatic host highly susceptible to infections by waterborne pathogens since the olfactory pathway has direct access to the brain, bypassing the brain blood barrier that protects the brain from systemic pathogens. Some pathogens have been shown to use the olfactory epithelium as a portal of entry to infect the nasal cavity and the CNS (Sepahi et al., 2019). To combat potential infections, the nasal cavity, olfactory bulb and higher regions of the brain of fishes are equipped with a specialized immune system (neuroimmune) similar to that seen in mammals (Verburg-van Kemenade, Stolte, Metz, & Chadzinska, 2009). The defense mechanisms employed by the neuroimmune system have been elucidated in several studies. First, early research examined cellular inflammatory changes in the olfactory bulb of mice following vesicular stomatitis virus (VSV) infection (Bi, Barna, Komatsu, & Reiss, 1995; Durrant, Ghosh, & Klein, 2016). This research showed an increase in the production of nitric oxide and the major histocompatibility complex in the olfactory bulb, which coincided with decreased viral titers in tissue homogenates (Bi et al., 1995; Durrant et al., 2016). Additionally, multiple studies utilizing viruses, such as VSV or influenza, have demonstrated increased expression of various innate cytokines, including interleukin 12, tumor necrosis factor (TNF- α) and interleukin-1 β within the OB (Durrant et al., 2016). These innate cytokines are secreted as an immune response to restrict replication of viruses within the CNS (Durrant et al., 2016). Cumulatively, evidence from these murine models has demonstrated that viruses that are first detected within the olfactory bulb can be quickly

cleared following increased expression of innate immune molecules. This result suggests that the olfactory bulb may offer an effective neuroprotective immunity to prevent anterograde transmission (from neuronal body to the axon end) of a virus to the brain (Durrant et al., 2016). The immune response of the olfactory bulb to viruses has been described recently in trout (Sepahi et al., 2019). However, the neuroprotective role of the olfactory bulb against bacteria has not been explored in fish and little is known about the exact underlying mechanism of neurotropic transmission.

In rainbow trout, recent literature has showed that neurotropic transmission, the infection of nervous cells, occurs through crypt cells. Crypt neurons are only known to express one type of odorant receptor, the vomeronasal receptor 1-like Ora4, which can be identified by its TrkA-like receptor immunoreactivity (Sepahi et al., 2019). TrkA is a high affinity receptor for the neurotrophin nerve growth factor which is responsible for mediating neural differentiation and avoidance of apoptosis (Catania et al., 2003; Sepahi et al., 2018). The presence of TrkA receptors has been described in the olfactory epithelium in mammals (Catania et al., 2003; Miwa et al., 2002). This receptor plays an important role in neuronal regeneration of the olfactory epithelium when cells are damaged or infected (Miwa et al., 2002). Thus, the TrkA-like receptors found in rainbow trout may serve a similar function as described in mammals. However, the TrkA-like receptor is susceptible to exploitation by pathogens due its proximity to the external environment. A recent study demonstrated that intranasal delivery of a virus resulted in a significant decrease in the number of TrkA-like receptor-expressing cells in the olfactory epithelium and a significant increase in the expression of pro-inflammatory cytokines (CCL19 and IFN) within 15 minutes (Sepahi et al., 2019). Furthermore, this research

demonstrated neuronal activation in the olfactory epithelium and the olfactory bulb by immunohistochemistry using p-ERK antibodies and electrophysiology. These results showed an increase in p-ERK-labeled cells in fish treated with Infectious Hematopoietic Necrosis Virus compared to the control. Moreover, these results were abrogated following pharmacological blocking of the receptors, thus indicating that INHV induces OSN activation in a TrkA-like receptor-dependent manner (Sepahi et al., 2019). Cumulatively, these results implicate olfactory sensory neurons in the orchestration of the nasal-neural immune response to rapidly remove pathogens from the olfactory epithelium. Thus, OSNs may play a more critical role in neural immunity than previously described and are critical for maintaining the integrity and functionality of the olfactory neuroepithelium.

Although viral entry in the CNS via OSNs and the subsequent antiviral immune response has been studied, significantly less is understood about how detection of bacteria is integrated within the CNS. Current literature has shown that mammals can directly detect bacteria by sensing bacterial toxins and metabolites (Yang & Chiu, 2017). Mammals, including humans and mice, may be able to smell bacteria by detecting N-formyl peptides via FPR G-protein coupled receptors (Yang & Chiu, 2017). Another study demonstrated that intranasal infection of *Listeria monocytogenes* in neonatal mice rapidly spread via OSNs to the CNS (Pägelow et al., 2018). This bacterial spread coincided with immune cell recruitment and cytokine infiltration in the OB and frontal lobe (Pägelow et al., 2018). Cumulatively, this research demonstrates that bacteria can enter the olfactory sensory neurons to reach the CNS. However, it is unknown if bacterial detection activates neural circuits involved the nasal-neuro immune response.

Additionally, it is unclear if the neural stimulation from the olfactory epithelium stimulates the secretion of neurosteroids, which have been shown to have neuroprotective benefits and mediate behavior.

1.3 The Role of Neurosteroids in Mediating Inflammatory and Behavioral Responses

Neurosteroids are steroids that are synthesized within the CNS *de novo* from cholesterol or by *in situ* metabolism of circulating steroids via steroidogenic enzymes (Do Rego et al., 2012). Steroidogenic enzymes are highly expressed in steroidogenic tissues, such as the ovary and testes, but are also present in other tissues like the brain (Diotel et al., 2018 ; Diotel et al., 2011a; Diotel et al., 2011b). *De novo* steroidogenesis from cholesterol is mediated by steroidogenic acute regulatory protein (StAR; Fig7), which is responsible for transporting cholesterol to the inner mitochondrial membrane (Bremer & Miller, 2014; Diotel et al., 2011b). Cholesterol derivatives are synthesized by two classes of steroidogenic enzymes: cytochrome P450s, which mediate hydroxylations and carbon-carbon bond cleavage reactions, or hydroxysteroid dehydrogenases that catalyze the dehydrogenation of hydroxysteroids (Bremer & Miller, 2014; Diotel et al., 2011b). The expression of P450 enzymes and hydroxysteroid dehydrogenases have been documented in the brain of zebrafish following reversed phase-high performance liquid chromatography (RP-HPLC) analysis (Bremer & Miller, 2014; Diotel et al., 2018). Biochemical studies have shown that the brains of adult zebrafish are able to convert cholesterol into pregnenolone in a rate-limiting reaction (Bremer &

Miller, 2014; Payne & Hales, 2004). Steroidogenic enzymes can then sequentially convert progesterone into a variety of steroids including 17-OH-pregnenolone, dehydroepiandrosterone (DHEA) through either the delta 4 pathway, which ends with androstenediol, or the delta 5 pathway which ends with androstenedione. From there, androgens including testosterone, dihydrotestosterone, 17 β -estradiol (E2) and estrone (E1) are synthesized as summarized in Fig 2 (Bremer & Miller, 2014; Diotel et al., 2011a; Payne & Hales, 2004).

In vertebrates, it has been shown that neurosteroids are involved in neurodevelopment, synaptic connectivity and neuroinflammation following brain injury (Bremer & Miller, 2014; Diotel et al., 2011b). Neurosteroids play an important role in modulating neural excitability by interacting with G protein-coupled cell surface receptors or by acting as a ligand and interacting with ligand gated ion channels on other neurons (Do Rego et al., 2012). A common feature of teleost fish brains is high aromatase expression in the brain (Diotel et al., 2011c). Aromatase converts androgens, such as testosterone, into estrogens, such as estradiol, which are known for having neuroprotective and anti-apoptotic properties (Coumailleau et al., 2015; Diotel et al., 2010). There are two structurally and functionally different isoforms of aromatase: aromatase A, found in the gonads, and aromatase B, found in the brain of teleost fish (Diotel et al., 2011a; Diotel et al., 2011b). Aromatase B activity has been detected in several regions of the brain including the olfactory bulb, hypothalamus, thalamus, preoptic area and telencephalon (Coumailleau et al., 2015; Pellegrini et al., 2016). Immunohistochemistry and *in situ* hybridization experiments localized aromatase B expression in regions populated with radial glial cells (RGCs), which persist throughout

life and act as neuronal stem cells in developing fish (Diotel et al., 2010). Research in zebrafish showed that inhibiting aromatase activity significantly decreased cell proliferation and migration of newborn neurons (Diotel et al., 2013; Siddiqui et al., 2016). Radial glial cells synthesize *de novo* a variety of other neurosteroids including progesterone, pregnenolone, DHEA and allopregnenolone. Pregnenolone has been reported to enhance neural growth and plasticity and can inhibit cell migration in zebrafish (Diotel et al., 2018 ; Diotel et al., 2013). DHEA and allopregnenolone are known to suppress the secretion of cytokines such as TNF- α and IL-6, thereby modulating the inflammatory response (Murugan, Jakka, Namani, Mujumdar, & Radhakrishnan, 2019). Collectively, these results demonstrate that neurosteroids play a significant role in maintaining brain homeostasis (Bremer & Miller, 2014; Diotel et al., 2011a; Payne & Hales, 2004).

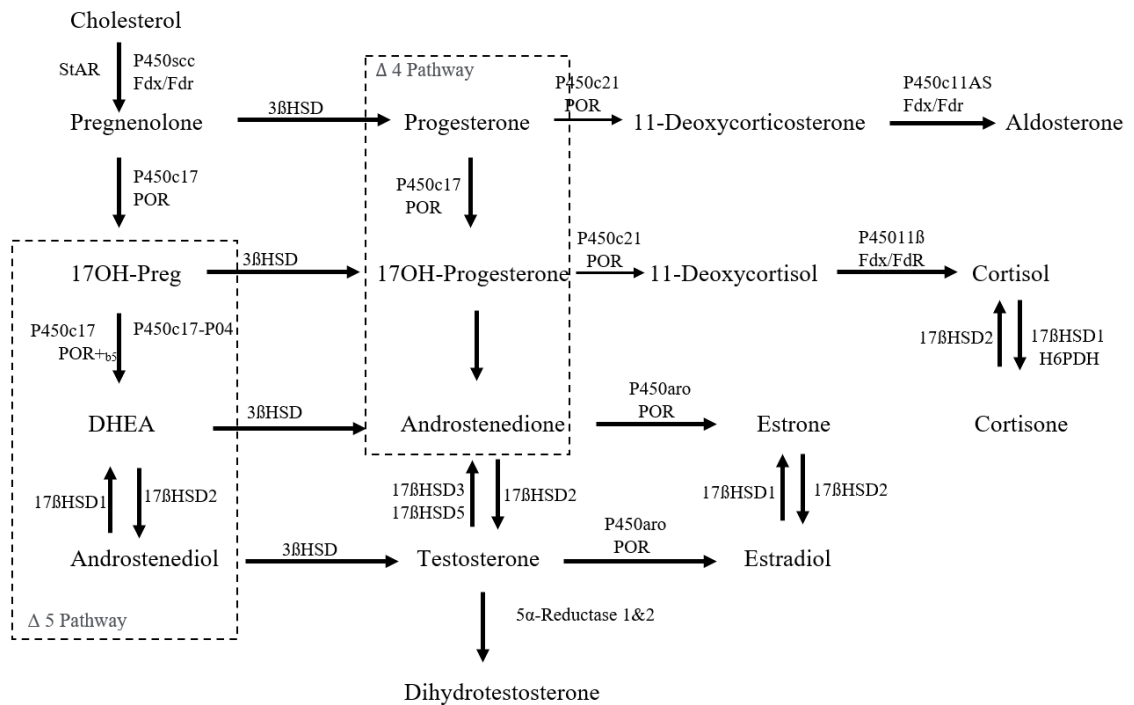


Figure 2. Summary of Steroidogenic Pathways. The first step in the steroidogenic pathway is the conversion of cholesterol to pregnenolone via P450scc. From there, steroid biosynthesis can proceed either

through the "delta-5" pathway or "delta-4" pathway. The former pathway begins by the synthesis of dehydroepiandrosterone (DHEA) from 17 α -hydroxypregnenolone and then the subsequent synthesis of androstenediol from DHEA. Both DHEA and androstenediol serve as metabolic precursors for several androgens including testosterone, dihydrotestosterone, estrone and estradiol. The latter pathway begins by the conversion of pregnenolone to progesterone, which acts as a metabolic intermediate for the eventual synthesis of corticosteroids (11-deoxycortisol, cortisol, and cortisone), mineralocorticoids (11-deoxycorticosterone, aldosterone), and androgens (androstenedione, etc.). Figure adapted from Fig 13.1 by Bremer & Miller, 2014.

1.4 Infectious Hematopoietic Necrosis Virus and *Yersinia ruckeri* in Aquaculture

Rainbow trout are a predominant species used in recreational fishing and provide sustenance to certain communities (Assefa & Abunna, 2018). However, their population is dwindling, and certain subspecies are currently on the endangered species list because of habitat degradation and disease (Breyta et al., 2017). Disease is a major problem in aquaculture and investigating new preventative measures can significantly reduce the prevalence of infection in fish. In 2019, the United States Department of Agriculture (USDA) reported 122.5 million trout sales totaling \$136.0 million. However, that same year 32.0 million trout were lost, with disease accounting for 88% of total loss. Two pathogens, Infectious Hematopoietic Necrosis Virus (IHNV) and *Yersinia ruckeri*, are considered detrimental to aquaculture due to the lack of available treatment and manufacturers' decision to control these infections by culling, resulting in large financial loss.

IHNV is negative-sense, single-stranded RNA virus belonging to the *Rhabdoviridae* family (Yong et al., 2019). This virus is characterized by its bullet-shaped morphology and measures 150-190 nm in length and 65-75 nm in width (Yong et al.,

2019). *Y. ruckeri* is a gram-positive, rod-shaped bacterium of the *Yersiniaceae* family (Wrobel, Leo, & Linke, 2019). This bacterium is rounded and measures 0.75 μm in diameter and 1-3 μm in length (Wrobel et al., 2019). Although IHNV and *Y. ruckeri* are vastly different pathogens, outbreaks of both pathogens have significant economic and ecological impacts. Therefore, several preventative measures, such immersion and oral vaccination, are undertaken to reduce infection rates and severity (Assefa & Abunna, 2018). Additionally, nasal vaccination, a novel area of research, has been successful in controlling aquatic infections and been shown to be effective using live attenuated IHNV vaccine and enteric red mouth bacteria vaccine (S. LaPatra, Kao, Erhardt, & Salinas, 2015).

Although IHNV and *Y. ruckeri* are both present in the aquatic environment, their modes of infection differ. IHNV has been shown to enter via the olfactory organ whilst *Y. ruckeri* has been primarily shown to enter via the gills (Guijarro, García-Torrico, Cascales, & Méndez, 2018). Specifically, IHNV has been shown to enter the nasal cavity by neurotropically interacting with OSN receptors in the olfactory epithelium (S. E. LaPatra et al., 1995; Sepahi et al., 2019). This interaction is transduced into an electrical signal that travels to the olfactory bulb and ultimately activates the nasal immune response to prevent further infection in the CNS (Sepahi et al., 2019). However, it is unclear if OSNs can also detect bacteria, and we currently lack information regarding the higher levels of integration within the nervous system of rainbow trout when exposed to microbes (viruses and bacteria).

2. THESIS GOAL

Although neurocircuits have been extensively studied in higher vertebrates, much less is known about neurocircuits in fish. Specifically, research focused on the neurocircuitry involved in pathogen detection via olfaction, across vertebrates, remains inconclusive. It has been shown that the neural-immune response can be activated by IHNV through the olfactory sensory neurons. However, it is unknown if bacteria also activate OSNs or if they induce the same effects. Despite this, research suggests that bacteria and/or bacterial metabolites activate neural circuits that mediate behavior and cognitive moods (such as anxiety or depression) in mammals (Carabotti, Scirocco, Maselli, & Severi, 2015). Thus, this data leads us to investigate if bacteria also activate neural circuits through the sensory neurons of the olfactory system. Moreover, we are unsure which biochemical elements (hormones, neurotransmitters, neurosteroids, etc.) are responsible for modulating these neural circuits. Additionally, it is unknown how these neural circuits integrate in specific physiological processes such as the immune response or regulating behaviors in an organism.

Olfactory signals are integrated within various regions of brain, including the telencephalon and hypothalamus, which regulate neurosteroid production and concomitant behavior. In fact, neurosteroids act as neuromodulators in synaptic transmission and have been documented to induce various behaviors in vertebrates (Heimovics, Trainor, & Soma, 2015; Kavaliers, Bishnoi, Ossenkopp, & Choleris, 2021). Thus, we hypothesize that bacterial activation of OSNs induce neurosteroid synthesis which in turn mediates behavioral changes.

The overarching goal of this study is to determine the olfactory-immune neural

circuit involved in pathogen detection as well as identifying the neurohormones that mediate physiological and behavioral changes. I hypothesize that IHNV and *Y. ruckeri* are detected by different subsets of crypt cells, and the information about their presence is integrated within different areas of the brain. Furthermore, I theorize that the main neuromodulators in olfactory immune process are neurosteroids, independent of the pathogen odorant. Finally, I speculate that pathogen odorants elicit an avoidance swimming behavior. Consequently, I expect that pathogens can be detected through olfactory neurons in trout, and this detection is integrated within the brain to trigger physiological and behavioral changes. Therefore, to test our hypothesis we designed three main objectives:

3. OBJECTIVES

3.1 Tracing OSNs from the Olfactory Rosette to the Brain in Rainbow Trout

Rainbow trout will be intranasally exposed to IHNV or *Y. ruckeri* (mixed with Alexa Fluor 568) for 1,4,7, or 14 days. Trout will then be euthanized using MS-222 and the heads will be fixed in PFA for 24 hours. The olfactory organ and brain will then be transferred to sucrose for 24 hours and subsequently cryosectioned at 10 μm .

Visualization of fluorescence within cells in both tissues will be done using a fluorescent microscope.

3.2 Quantifying Neurosteroids in the Olfactory Organ and CNS of Rainbow Trout after Nasal Exposure to Inactive Pathogens

Rainbow trout will be exposed to IHNV for 24 hours and 4 days and *Y. ruckeri* for 15 minutes, 4 hours, 24 hours, and 14 days. Neurosteroids will be extracted by using solid phase extraction and quantified by liquid chromatography-mass spectrometry (LC-MS) or enzyme-linked immunosorbent assays (ELISA).

3.3 Behavioral Assessment of Rainbow Trout to *Y. ruckeri*

Rainbow trout will be exposed to three cues (food odor, inactivated bacteria, and solvent control) and their behaviors will be assessed. The food cue will serve as a positive control in which we expect to see attractive behavior. The second cue, *Y. ruckeri*, will be used to determine if fish avoid bacteria when exposed and formaldehyde will be used as a positive control for avoidance behavior.

4. MATERIAL AND METHODS

4.1 Fish

Rainbow trout (0.15 g) were obtained from the hatchery, Troutlodge INC (Missouri). Upon arrival, the trout were placed in an aerated stream system with recirculating water that was maintained between 14.8° to 15.8°C. Fish were fed twice a day with commercial pellets (Zeigler Finfish Starter Meal 0.4 - 0.6 mm) until they were the optimum size for experiments (5.69 g ± 0.29 g SEM) and then switched to a once-a-day feed schedule. Weekly water changes were done to maintain levels of ammonia, nitrate, and nitrite (0 to 0.01 ppm). Texas State IACUC approval code for fish was 201610209606.

4.2 IHNV Vaccine

Stocks of live, attenuated IHNV vaccine (2×10^8 PFU/mL) were prepared from the IHNV strain 220-90 in epithelioma papulosum cyprini cells (EPC) from common carp, *Cyprinus carpio* as explained in LaPatra et al. (1995).

4.3 *Y. ruckeri* Vaccine

Y. ruckeri was grown from stock culture on tryptic soy agar and incubated at 25°C for 24 hours. It was then inoculated into 10 mL nutrient broth and incubated at 25°C for 24 hours, subsequently serially diluted and then replated on TSA for 24 hours. Plates with between 20-200 colonies were counted and the CFUs were calculated (# of colonies x dilution factor)/ volume of culture plate. After the CFU was determined from the stock, the bacteria were serially diluted to the desired concentration of 2×10^9 CFU/mL. The bacteria were then inactivated by incubation with 1% formaldehyde for 2 hours at room temperature. The formaldehyde inactivated bacteria were then washed three times with

DI water by centrifugation (14,000 x g, 10 min) and resuspended in water to attain a concentration of 2×10^9 CFU/mL.

4.4 Chemical Solutions

We used Alexa Fluor 488 conjugated to 3 kDa dextran, Alexa Fluor 555 conjugated to 10 kDa dextran, Alexa Fluor 568 conjugated to 10 kDa dextran or Alexa Fluor 647 conjugated to 10 kDa dextran (Table 1; Thermo Fisher Scientific). Stock fluorescent solutions for IHNV and *Y. ruckeri* were made and diluted using distilled water to the desired concentration as listed in Table 2. Final concentrations of fluorescent solutions were 0.112 mg/mL, 0.126 mg/mL 0.01 mg/mL, and 0.45 mg/mL, respectively. The final tracing solution was then made by adding 1 mL of formalin killed *Y. ruckeri* or 1 mL inactivated IHNV to 10 mL of fluorescent solution (1:11 solution).

Table 1. Summary of Alexa Fluor-Dextran Properties

Alexa Fluor	Dextran Molecular Weight	Excitation (nm)	Emission (nm)	Emission Color	Filter
488	3 kDa	490	525	Green	GFP
555	10 kDa	555	580	Orange	TRITC
568	10 kDa	578	603	Red	DSRED
647	10 kDa	650	665	Red	Cy5

4.5 Nasal Exposure of Inactivated IHVN and *Y. ruckeri* for Histology and

Neurosteroid Extractions

Rainbow trout were kept under a continuous flow of anesthetic (MS-222; 0.1 g/L) delivered orally via a tube. The olfactory rosettes were then flushed with the various vaccine solutions for 1-2 minutes at 6 mL/min (Table 3). After each exposure, the rosettes were rinsed for 1-5 minutes with charcoal filtered tap-water to remove residual

solution, and then fish were placed in their tank for their respective incubation periods of 24 hours, 4 days, and 14 days. Flow rate of dye and vaccine solutions was maintained at 6 mL/min.

For the neurosteroid experiments trout were temporarily anesthetized as described before and 30 μ L of IHVN (PBS for control) or formaldehyde-killed *Y. ruckeri* (formaldehyde for control) was pipetted into both olfactory cavities. *Y. ruckeri* treated fish were returned to a tank for the following incubation periods: 15 minutes, 4 hours, 24 hours, and 14 days. IHNV-treated fish were returned to their tank for 15 minutes. Treated and control groups between experiments were kept in separate tanks and consisted of 10 fish.

4.6 Tissue Collection and Histology

Following the respective incubation period, rainbow trout were anesthetized using Tricaine mesylate (MS-222) at a concentration of 0.1 g/L. For histology, fish were sacrificed, by severing the spinal cord behind the head, and fixed in 4% paraformaldehyde (PFA) for 18 hours with the nares and brain exposed. Samples were then transferred to 30% sucrose for cryopreservation for 24 hours, and then brain and nose tissues were dissected out. Samples were cryosectioned, counterstained with DAPI, and visualized using a corresponding filter on fluorescent microscope (Table 1).

For neurosteroids extractions, the olfactory epithelium, olfactory bulb, and remaining brain were individually collected and snap frozen in liquid nitrogen until further use.

4.7 Steroid Extractions

Neurosteroids extractions were quantified from the olfactory bulb and brain of trout following intranasal exposure to IHNV. Likewise, neurosteroid extractions were quantified from olfactory epithelium, olfactory bulb, and brain of trout following intranasal exposure to *Y. ruckeri*. All samples were weighed prior to extractions and subsequently homogenized with 1 mL of 70% ethanol and then centrifuged at 9000 rotations per minute for 1 minute. Supernatant was transferred to a new tube and evaporated overnight. Homogenate was then resuspended in 1 mL of 1:9 methanol: phosphate buffer.

For IHNV samples, 100 μ l aliquots of each sample were transferred to a new tube and extracted for conjugated forms. Samples were evaporated overnight and then resuspended in 1 mL of ethyl acetate and trifluoroacetic acid (TFA) and left overnight at 40°C. The ethyl acetate was evaporated and 500 μ L of acetate mix and 3 mL of ether was added to each sample. The acetate mix was comprised of 5 mL of stock A (8.2 g sodium acetate per 100 mL distilled water) and 1.4 mL of stock B (8.5 mL HCl per 100 mL distilled water). Samples were mixed for 10 minutes and then sat at room temperature for 10 minutes. Following this, samples were dipped in liquid nitrogen and the ether was then transferred to glass vials for evaporation in a 40°C bath. 0.5 mL of methanol was added to vials in the bath, mixed and then transferred to new Eppendorf tubes and stored at -80°C for further processing.

The remaining 900 μ L samples were processed by Sep-pack extraction using bond elute C18 cartridges. The SPE cartridges were conditioned with 2 mL methanol and 4 mL water. Samples were loaded and the cartridges were rinsed with 2 mL water and

subsequently eluted with 1.5 mL of methanol. The flow rate was maintained at 1 mL/minute. The eluate was then collected in 1.5 mL centrifuge tubes and evaporated. Lastly, extracts were transferred to new tubes with 0.5 mL of 100% ethanol for quantification by ultra-high performance liquid chromatography tandem mass spectrometry (UPLC-MS/MS) in the Metabolomics Core Facility at University of California at Riverside.

For *Y. ruckeri* samples, 1:9 samples were processed as described above and then transferred to new tubes with 1 mL PBS and stored in -20°C. *Y. ruckeri* extracts were quantified using an enzyme-linked immunosorbent assay (ELISA; Cayman Chemical, Inc).

4.8 Enzyme-Linked Immunosorbent Assay (ELISA)

Estradiol, progesterone, and cortisol were quantified in *Y. ruckeri* treated tissues using a specialized ELISA kit. First, the standard curve was prepared by serially diluting steroid stock solution with ELISA buffer as instructed. Next, 100 µL of ELISA buffer was added to non-specific binding wells (NSB) wells and 50 µL was added to maximum binding (Bo) wells. 50 µL of the standard was then added from the lowest concentration to the highest in designated wells. Finally, 50 µL of samples, steroid tracer and steroid ELISA antibody was added to the wells as instructed. The microplate was then covered and incubated overnight at 4°C. Following incubation, wells were aspirated and rinsed five times with wash buffer. Ellman's reagent (200 µL) was then added to each well, and 5 µL of tracer was added to the total activity (TA) wells. The plate then developed in the dark for 60, 90 and 120 minutes. Readings were taken after each period using a spectrophotometer to measure absorbance. A two-way analysis of variance (ANOVA)

was conducted to estimate differences among treatments in IHNV- and *Y. ruckeri*-treated groups. The critical value for statistical significance was taken as $p < 0.05$. Statistically significant factor effects are denoted by asterisks. Data graphs were plotted as mean \pm standard error of the mean values using the GraphPad Prism software.

4.9 Behavior

Two-choice maze behavioral assays were used to evaluate behavioral changes in response to food, bacteria, and formaldehyde cues (Bett, Hinch, & Yun, 2016). The two-choice maze was constructed using clear, acrylic plastic sheets with dimensions measuring 122 mm in length, 30.5 mm in width and 26 mm in height (Fig. 3 A). Inflow was created and maintained using a submersible water pump (Pondmaster™ POND MAG3) in a tank adjacent to the maze and a multichannel peristaltic pump (Cole-Parmer® Catalyst™ Masterflex FH Series) was used to release both cues (Fig. 3 A, B). A mesh barrier (1-3/4 x 1-3/4) was placed in each odor channel (29 mm away from the end) for even laminar flow and dispersion of cues. Finally, a dye test was conducted to ensure that there was no overlap of flow between the two channels (Fig. 3 C).

Fish were not fed the morning of experiments to increase their response to the cue. Behavioral assay consisted of four phases: 1) 10 minutes for acclimation in arena, 2) 10 minutes for exploration of both channels to establish channel preference, 3) 10 minutes of re-acclimation in arena, 4) 10 minutes for exploration to determine preference channel when exposed to cue. Time (seconds) spent in each channel was recorded during the exploration and cue phase. The experimental and control cues were released at the 7th minute during the re-acclimation phase via a peristaltic pump set at 150 RPM. Food cue was added in the chamber opposite of the preferred side, while the bacteria cue and

formaldehyde cue were added in the preferred side. A control cue (distilled water) was released in the opposite channel to the experimental cues. Food odor was made using 1g of commercial food per liter of di-water the day before behavior experiments and filtered the day of trials. Bacteria cue was made by diluting 1 mL of 2×10^9 CFUs per liter of distilled water. Formaldehyde (37% stock) cue was made by diluting a solution of 0.1% into 1 liter of water. After completing each trial, the two-choice maze was drained and refilled.

The time spent in control and experimental chambers during each phase were measured, recorded, and organized as the following: BC = time spent in control chamber before odor release, BE = time spent in experimental chamber before odor release, AC = time spent in control chamber after odor release, AE = time spent in experimental chamber after odor release. An index of preference for each trial was calculated using the equation ($i = [AE/(AE+BE) - AC/(AC+BC)]$) and then evaluated using a Wilcoxon-signed rank test ($P < 0.05$). Graphs were constructed using Prism Software.

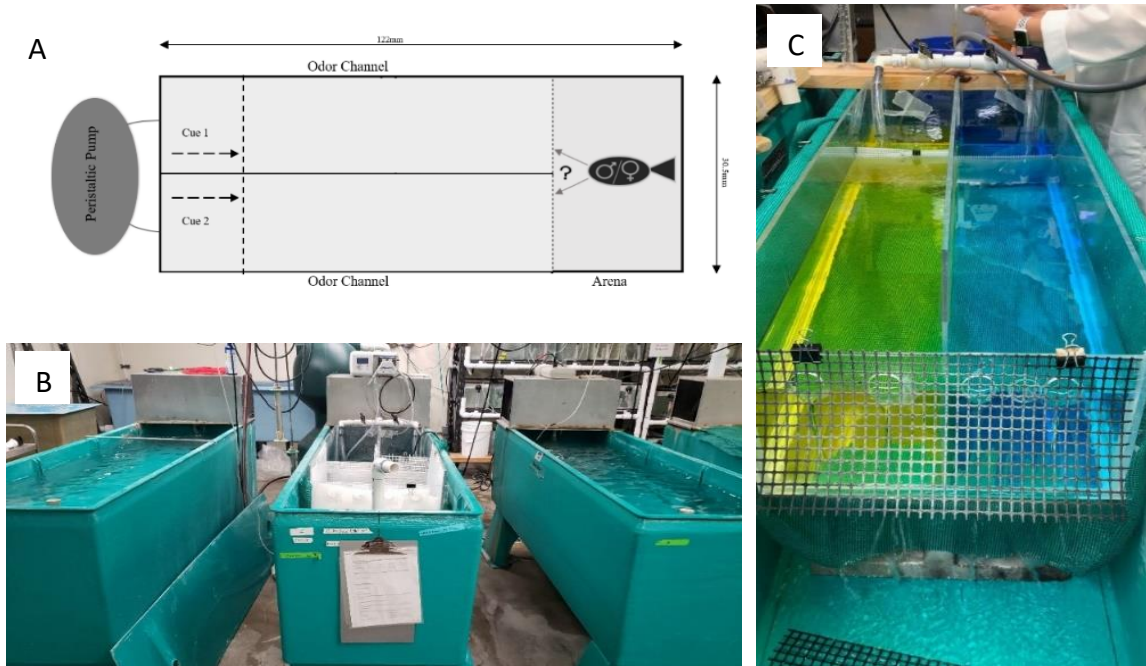


Figure 3. Two-Choice Maze for Behavioral Analysis of Rainbow Trout. (A) Schematic diagram of maze with dimensions. Maze was placed in tank and filled with water maintained between 14.5-15°C. (B) Inflow was created and maintained using a submersible water pump in tanks adjacent to the maze and a multichannel peristaltic pump was used to release control and experimental cues. (C) Dye test was conducted to ensure that there was no overlap of flow between both channels.

5. RESULTS

5.1 Histology: IHNV and *Y. ruckeri* Neurocircuit Tracing

Neurocircuit tracing was tested using a variety of Alexa fluor dyes, concentrations, exposure times, and vaccines (Table 2).

Table 2. Summary of Neurotracing Parameters Utilized for Histology.

Neurotracing Parameters					
Odorant	Exposure Time	Alexa Fluor	[Alexa Fluor]	Autofluorescence	Results
IHNV	1 min	488	0.112 mg/mL	Yes	Positive in OE
Media	1 min	488	0.45 mg/mL	N/a	Negative
Serine	1 min	647	0.45 mg/mL	N/a	Negative
<i>Y. ruckeri</i>	1 min	555	0.126 mg/mL	No	Positive in OE
<i>Y. ruckeri</i>	2 min	568	0.01 mg/mL	No	Positive in OE
<i>Y. ruckeri</i>	2 min	568	0.01 mg/mL	No	Positive in OE and OT

We visualized fluorescent, oval shaped cells near the apex of the epithelium in fish intranasally exposed to IHNV mixed with Alexa fluor 488 conjugated to 3 kDa dextran for 1 minute (Fig. 4B). However, significant autofluorescence made it difficult to identify and distinguish individual OSNs from one another and other cells in the epithelium, prompting us to try other types of Alexa fluor-conjugated dextrans that be detected with less background autofluorescence.

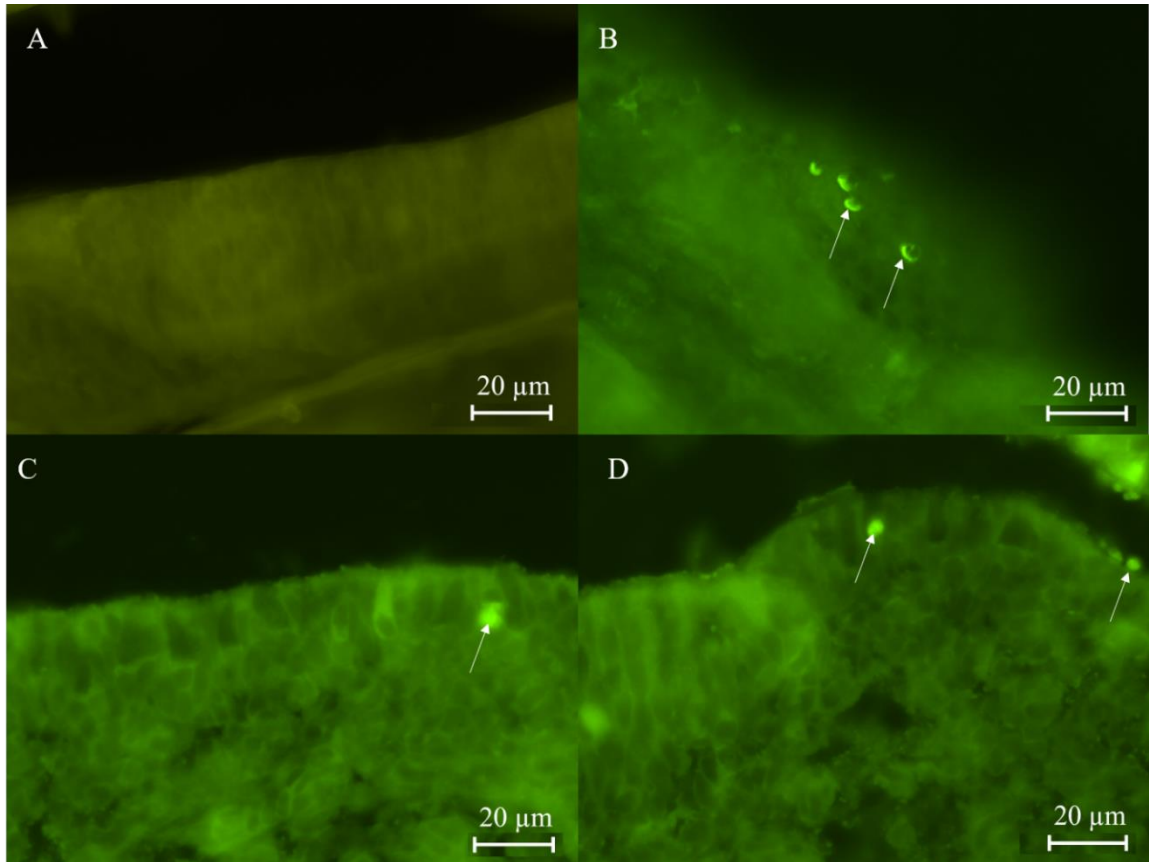


Figure 4. Fluorescence Micrograph of Olfactory Epithelium Exposed to IHNV and Media. Rainbow trout were intranasally exposed to IHNV mixed with Alexa fluor 488 conjugated to 3 kDa dextran (B) and media mixed with Alexa fluor 488 conjugated to 3 kDa dextran (C, D). Samples were cryosectioned at 15 μm and visualized with GFP filter. (A) No fluorescence was detected in control. (B) Fluorescent crypt-like cells were observed near apical surface of epithelium as shown by arrows. (C, D) Autofluorescence was emitted from various artifacts in media sections as shown by arrows.

To identify the most effective Alexa flour, fish were then intranasally exposed to *Y. ruckeri* vaccine mixed with Alexa fluor 547 or 555. Results were inconclusive in tissues exposed to Alexa fluor 547 and *Y. ruckeri* (data not shown). However, we observed that exposure to Alexa fluor 555 and *Y. ruckeri* caused staining of two classes of sensory neurons in the olfactory epithelium 24 hours after exposure: a globular shaped cell near the apical surface of the OE (Fig. 5B) and a tubular-like cell with a process that

extends towards the surface. The somata of the tubular cell resided in deeper layers of the epithelium (Fig. 5D). Exposure to the dye without *Y. ruckeri* did not result in staining of cells in the epithelium (Fig. 5A, C). Clear visualization of cells from these results indicates potential use of Alexa fluor 555 for further experiments, however we wanted to determine the efficacy of Alexa Fluor 568.

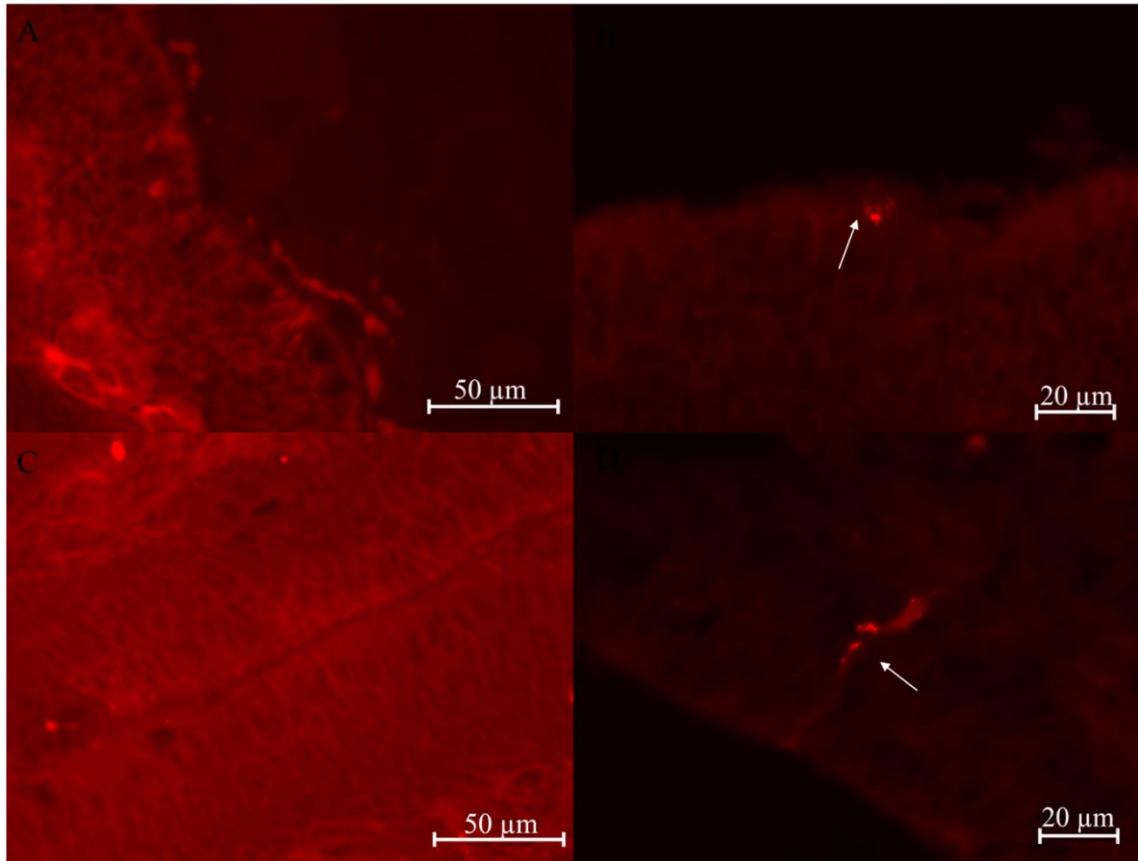


Figure 5. Activated Olfactory Sensory Neurons Following Intranasal Delivery of *Y. ruckeri*. Olfactory epithelium exposed to *Y. ruckeri* mixed with Alexa fluor 555 24 hours after exposure. Tissues were cryosectioned at 10 μm and viewed using DSRED filter. (A) Apex of control. (B) Fluorescent crypt-like neuron was visualized near the apex of the epithelium. (C) Lamellae of control. (D) Fluorescent dendritic process was detected along lamellae of epithelium indicating detection through ciliated neurons.

Fish were then exposed to either a PBS or water-based *Y. ruckeri* vaccine mixed with Alexa fluor 568 for 1 minute. Results showed a high density of fluorescent stained

cells throughout the lamellae (Fig. 6B). These cells are thought to be ciliated neurons due to their elongated process that extends towards the surface. However, a smaller globular cell, thought to be a crypt or kappe neuron, was observed near the apical surface (Fig. 6B). In contrast, a singular cell was detected in the lamellae of tissues treated with the PBS-*Y. ruckeri* vaccine. No fluorescent cells were detected in either control (Fig. 6A, C).

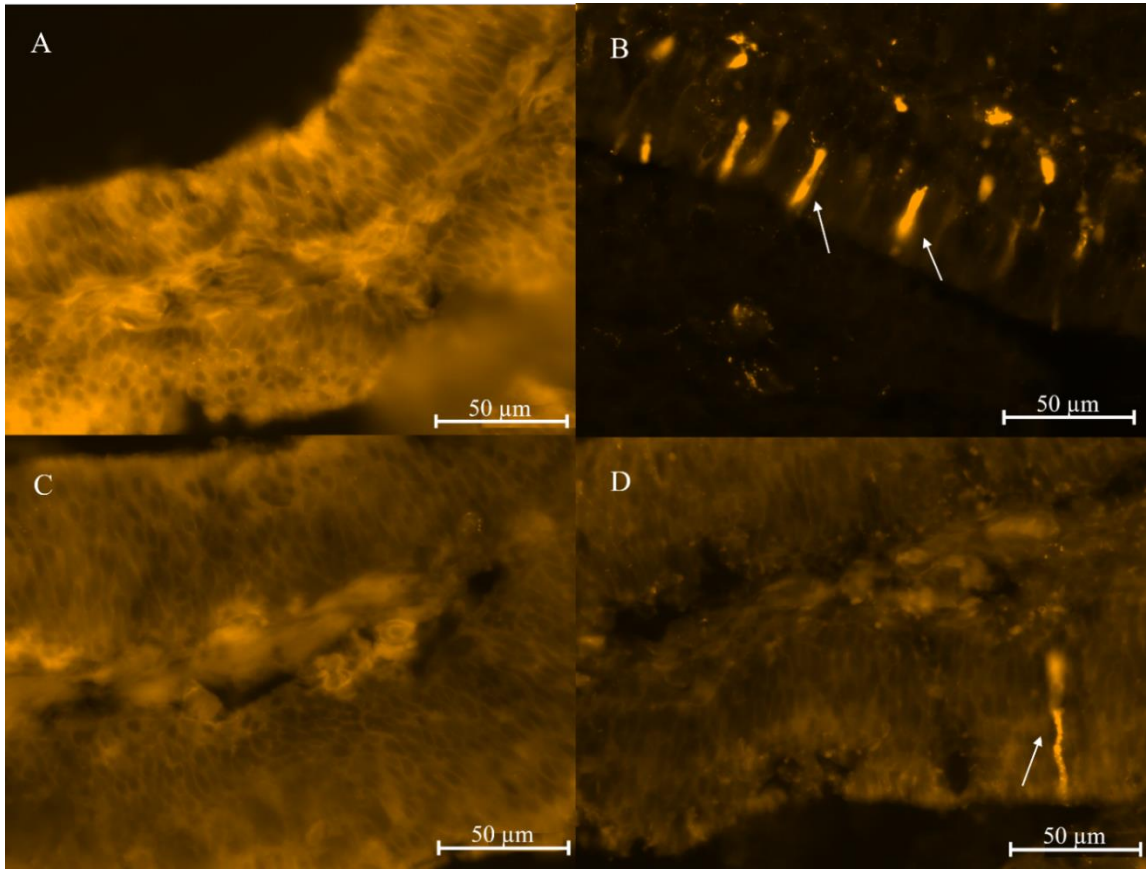


Figure 6. Olfactory Response to PBS and Water-Suspended *Y. ruckeri* vaccines. Trout were intranasally exposed to either a PBS-suspended *Y. ruckeri* vaccine mixed with Alexa fluor 568-conjugated to 10 kDa dextran or a water-suspended *Y. ruckeri* vaccine. Images were captured with DSRED filter. (A) Olfactory epithelium (OE) flushed with PBS and Alexa fluor 568. (B) OE flushed with water-suspended *Y. ruckeri* vaccine. Fluorescent ciliated cells were visualized throughout the epithelium, indicating endocytosis of dye. (C) OE flushed with water and Alexa fluor 568. (D) OE flushed with PBS-suspended *Y. ruckeri* vaccine. Fluorescent ciliated cell was visualized in OE.

Similar results were seen in a subsequent neurotracing. Exposure to Alexa fluor 568 and *Y. ruckeri* caused fluorescent staining of cells near apical surface of the OE 24 hours post exposure to the pathogen plus dye (Fig. 7 G, J). Cells had a globular-like morphology with a process extending towards the basal surface of the epithelium. Their apical position and axonic process indicates that they may be crypt sensory neurons, thus implying activation of cells in the periphery. Furthermore, fluorescent staining was not seen in the brain of treated tissues nor in control samples that were exposed to the dye without *Y. ruckeri* (Fig. 8 A, C). In contrast, after a 14-day exposure period to *Y. ruckeri* and Alexa fluor 568, fluorescent OSNs were not observed. Despite this, fluorescent staining was detected in the deep layer of the optic tectum. This was noted in both anterior and lateral regions of the OT (Fig. 8G-I).

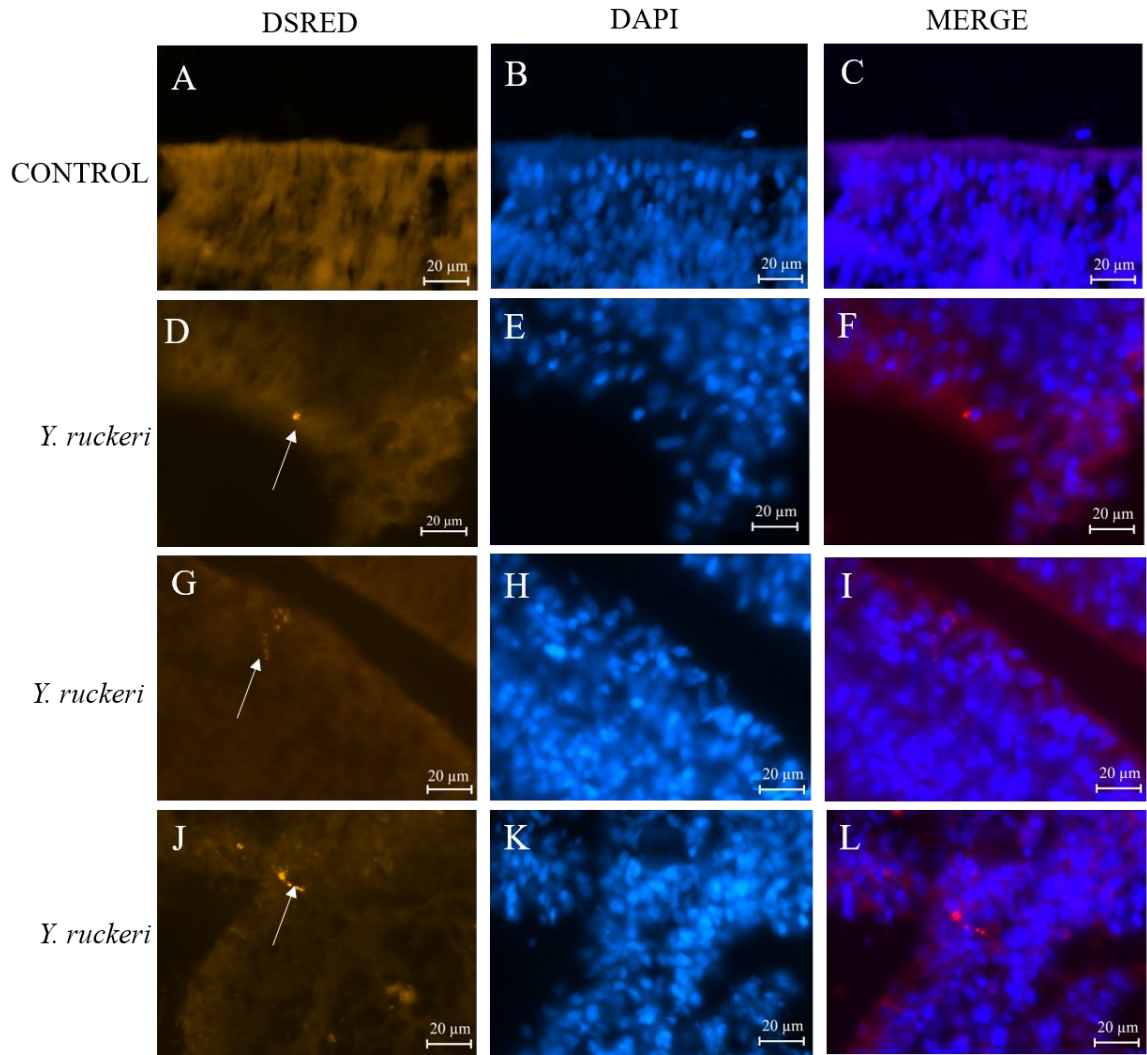


Figure 7. *Y. ruckeri* Activates Crypt-like Cells in the Olfactory Epithelium. Fluorescent micrograph of olfactory epithelium exposed to *Y. ruckeri* mixed with Alexa 568 (excitation 578, emission 603) after 24 hours. Images were captured with DSRED and DAPI filter and then superimposed. (A, B, C) Control images of lamellae of epithelium. (D, G, J) Images illustrating fluorescent crypt-like cells (white arrows) near the apex of the epithelium. Axonic projections extend to deeper layers of epithelium, as shown by arrows. (E, H, K). DAPI stained nuclei. (C, F, I, L) Superimposed images of fluorescent stained cells and DAPI images.

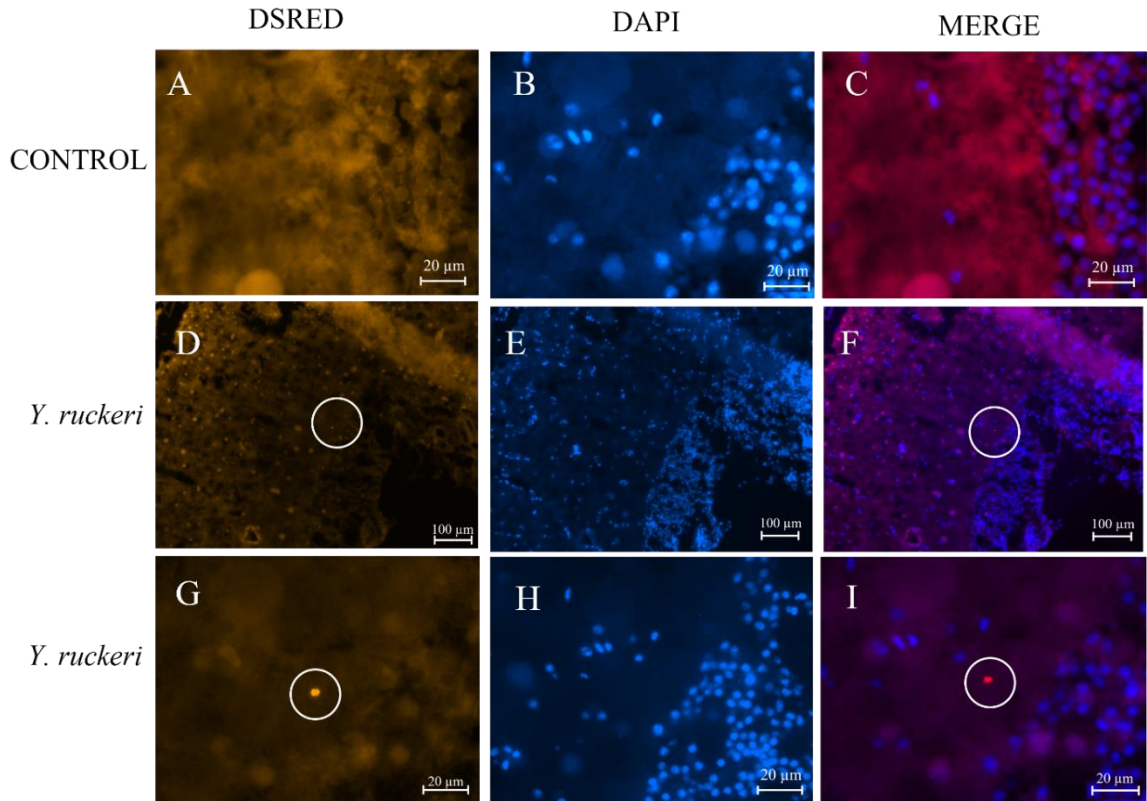


Figure 8. Intranasal Delivery of *Y. ruckeri* Traced to Higher Regions of the Brain. Fluorescent micrograph of optic tectum 14 days after intranasal exposure to *Y. ruckeri* mixed with Alexa fluor 568 (excitation 578, emission 603). Tissue was counterstained with DAPI for visualization of nuclei. Imaging was captured with DSRED (A, D, G) and DAPI (B, E, H) filter and subsequently merged (C, F, I). Fluorescence was detected in deep layer of optic tectum (D, G, F, I). No fluorescence was observed in the control (A, C).

5.2 Biochemical Analysis of Neurosteroids

We quantified several neurosteroids in OB and rest of brain (estradiol, androstenedione, testosterone, sulfated progesterone, cortisol, and sulfated cortisol) after exposure to IHNV. Differences in neurosteroid concentrations between control and IHNV 15 min after intranasal delivery were found in both the OB and rest of brain (Fig.9). Estradiol and androstenedione were the neurosteroids with highest concentrations

in both the OB and the rest of brain and seemed to be modulated by treatment. Estradiol was significantly higher in the OB (241.0 pg/g of tissue), compared to the control (98.2 pg/g of tissue). In the rest of brain, estradiol concentration in the control was 638.0 pg/g of tissue while the treated concentration was 456.0 pg/g of tissue. In contrast, androstenedione was higher in both the OB (75.9 pg/g of tissue) and rest of brain (344.0 pg/g of tissue) in the control, compared to treated (70.0 pg/g of tissue and 24.9 pg/g of tissue, respectively). Testosterone was also modulated by treatment; the concentration in the rest of the brain was 68.0 pg/g of tissue in IHNV treated fish, compared to the control 29.0 pg/g of tissue. Testosterone was undetectable in the control OB but present in IHNV treated fish (23.8 pg/g of tissue). Lastly, sulphated progesterone, cortisol, and its sulphated form seems to be present in the rest of brain, but they were not modulated by treatment.

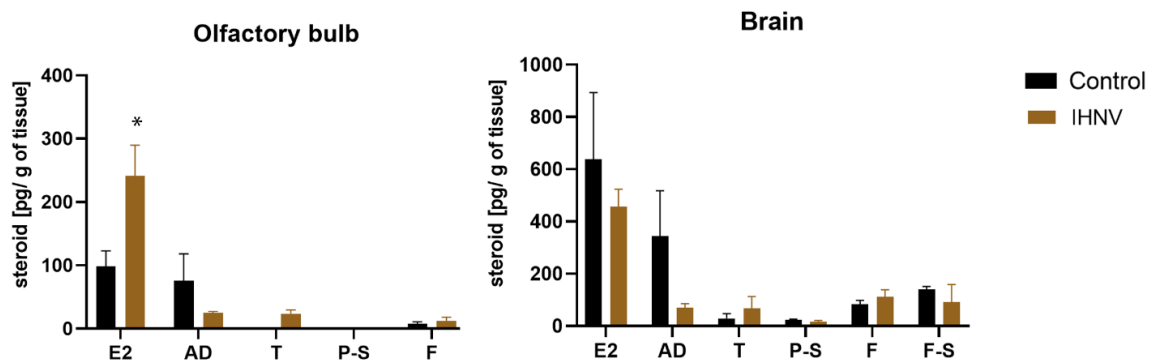


Figure 9. Olfactory Detection of IHNV Modulates Neurosteroids Concentration in the Olfactory Bulb and Brain. Intranasal exposure to IHNV resulted in an increase of estradiol (E2), testosterone (T), and cortisol (F), and a decrease in androstenediol (AD) in the olfactory bulb compared to the control. Comparatively, there was a decrease in estradiol and sulfated-cortisol (F-S) in the brain compared to the control. Asterisk denotes significant difference between vaccine and control treatments. N = 7

For the *Y. ruckeri* experiment, differential changes in cortisol, estradiol, and

progesterone were seen across tissues and time after treatments with the vaccine (Fig. 10-12). Within the OE, we detected a significant difference ($p < 0.05$) in cortisol and estradiol across time (Fig. 10). In contrast, there was no significant difference of progesterone across time. There was also a significant difference in neurosteroid concentration due to vaccine treatments. At 14 days, cortisol (10.95 pg/mg of tissue) was significantly lower in *Y. ruckeri*-treated fish compared to the control (78.76 pg/mg of tissue). Estradiol (26.06 pg/mg of tissue) was significantly lower after 15 minutes in *Y. ruckeri*-treated fish compared to the control (391.0 pg/mg of tissue). Moreover, there was a significantly higher concentration of progesterone (174.83 pg/g of tissue) in *Y. ruckeri*-treated fish after 4 hours compared to the control (26.5 pg/g of tissue).

Within the OB, there was a significant difference ($p < 0.05$) across time treatments but there was not significant difference between vaccine treatment and control for any the neurosteroids (Fig.11). However, there were differences in neurosteroid content due to vaccine exposure. Lower concentrations of cortisol (5.65 pg/mg of tissue) and progesterone (1.6 pg/mg of tissue) were observed after 15 minutes in the *Y. ruckeri*-treated fish compared to the control (22.8 pg/mg of tissue and 1.9 pg/mg of tissue, respectively). There was also a higher concentration of estradiol after 15 minutes and 4 hours compared to the control.

Lastly, within the rest of brain we detected a significant difference ($p < 0.05$) of cortisol and estradiol concentration, but not progesterone, across time (Fig.12). Neurosteroid concentration was lower at 15 minutes in the control compared to *Y. ruckeri*-treated fish. However, after 4 hours, a higher concentration of neurosteroids were detected in *Y. ruckeri*-treated fish. After 24 hours and 14 days, the concentrations of

neurosteroids were low and did not statistically change between vaccine treatments.

We also found a significant difference of neurosteroid concentration due to vaccine treatments. Cortisol (4.9 pg/mg of tissue) was significantly higher after 4 hours in treated samples compared to the control (9.08 pg/mg of tissue) and estradiol (5.50 pg/mg of tissue) was significantly lower after 15 minutes in *Y. ruckeri* samples, compared to the control (55.9 pg/mg of tissue). However, neurosteroid concentration in the rest of brain was relatively low compared to the OE and OB.

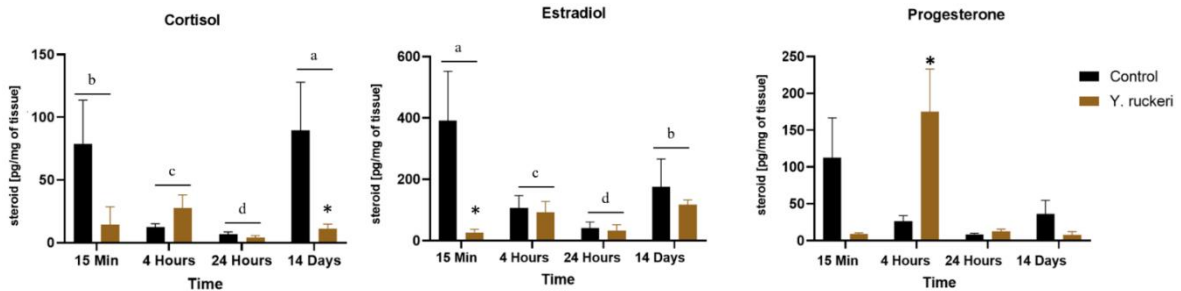


Figure 10. Characterizing the Presence of Neurosteroids in Olfactory Epithelia after Intranasal Delivery of *Y. ruckeri*. Concentrations of cortisol (F), estradiol (E2) and progesterone (P) were modulated in the olfactory epithelium. Estradiol was significantly ($p = 0.003$) higher in *Y. ruckeri* treated fish after 15 minutes. Progesterone was significantly ($p = 0.004$) higher after 4 hours and cortisol was significantly lower ($p = 0.003$) after 14 days. Letters denote significant difference across time and asterisks denote significant difference between vaccine and control treatments.

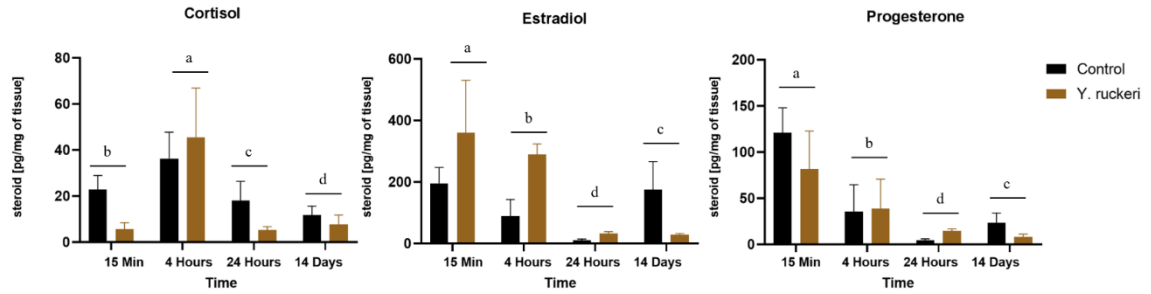


Figure 11. Olfactory Detection of *Y. ruckeri* Modulates Neurosteroid Concentrations in the Olfactory Bulb. Cortisol, estradiol, and progesterone concentrations significantly differed ($p < 0.05$) across treatment times but not between vaccine treatments in the olfactory bulb. Letters denote significant differences across time.

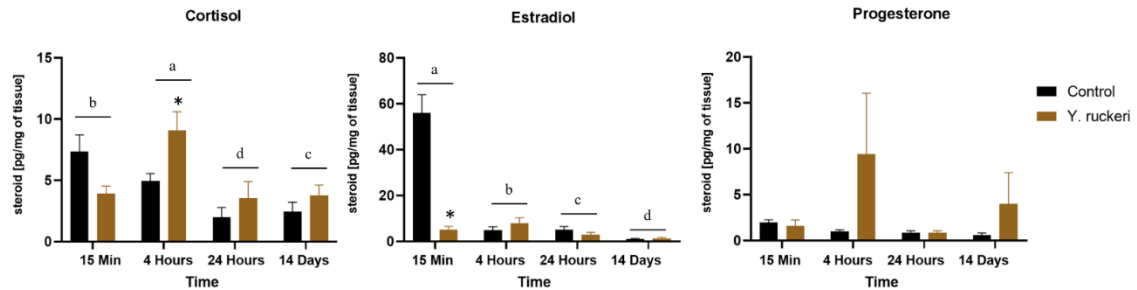


Figure 12. Neurosteroid Concentrations in the Rest of Brain Are Modulated after Olfactory Detection of *Y. ruckeri*. Estradiol was significantly ($p < 0.0001$) lower after 15 minutes, and cortisol was significantly ($p = 0.03$) higher after 4 hours in *Y. ruckeri*-treated samples. The trend of changes within both time stamps in brain paralleled findings within the olfactory epithelium. Letters denote significant difference across time and asterisks denote significant difference between vaccine and control treatments.

5.3 Behavior

Fish exhibited typical feeding behavior including searching, nibbling at the surface water, walls, and bottom floor of the maze when exposed to food. They showed significant preference when exposed to food (Wilcoxon-signed rank test $P < 0.05$, $p = 0.0163$), spending more time in the experimental channel (food cue) than in the control channel (water). Some fish ($n = 7$) showed immediate preference for the experimental

channel, spending 90% of their time there, while others ($n = 4$) showed a moderate preference, spending on average more than 50% of their time in the experimental channel. However, several fish ($n = 6$) did not show preference for food and spent most of their time in the control channel. Comparatively, when exposed to the bacteria cue, fish showed a significant preference (Wilcoxon-signed rank test $P < 0.05$, $p = 0.001$) for the control channel (water) than the experimental channel (bacteria cue). Several fish ($n = 13$) spent, on average, over 80% of their time in the control channel. Three fish spent more time in the experimental channel than the control channel, and two fish did not explore either channel, preferring the arena of the control overall.

Fish were re-trialed using the food cue to determine if their ability to detect odors was affected by previous bacterial cues. Overall, fish showed no significant preference when exposed to food and exhibited typical feeding behaviors. Moreover, there was a difference in the index of preference between pre- and post-bacterial cue trials; the index of preference dropped from 0.31 to 0.13. Finally, as a negative control, we tested the fish against formaldehyde to eliminate the possibility that residual formaldehyde, from the vaccine, could have affected behavior. Results showed no significant difference when exposed to formaldehyde. Conclusively, the positive index values for the food cue from the pre-bacteria cue, post-bacteria cue trials indicate attractive behavior. Formaldehyde cue did not demonstrate attractive or avoidance behavior. In comparison, when exposed to bacterial cues, rainbow trout demonstrated aversive behavior which is supported by the negative index value of -0.38.

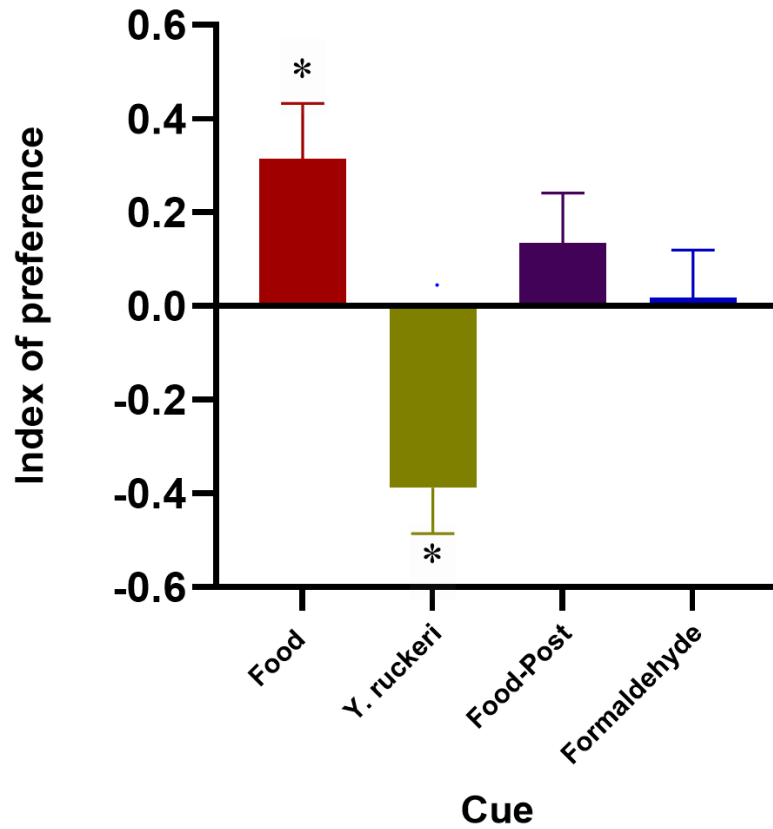


Figure 13. Two-choice Maze Behavioral Responses to Food, *Y. ruckeri*, and Formaldehyde. Rainbow trout were exposed to food cue (n = 18), *Y. ruckeri* (n = 18), food cue after *Y. ruckeri* trials (n = 9), and formaldehyde (n = 9). Index of preference ($I = [AE/(AE+BE)-AC/(AC+BC)]$) for all trials were calculated and then evaluated using a Wilcoxon-signed rank test ($\alpha = 0.05$). A positive index of preference indicates attractive behavior towards a cue, as shown by the food pre- and post-bacteria trials, while a negative index of preference indicates aversive behavior towards cue, as shown by *Y. ruckeri*.

6. DISCUSSION

Our results demonstrate that rainbow trout can detect *Y. ruckeri* via olfaction and subsequently modulate their behavior to avoid it. These findings support our hypothesis that IHNV and *Y. ruckeri* are detected by different subsets of crypt cells, and the information is integrated within different areas of the brain. Histological analysis of the olfactory epithelium demonstrated that ciliated-like OSNs are the prominent olfactory neuron involved in up-taking the fluorescent dextran in the presence of *Y. ruckeri*, 24 hours after exposure. Furthermore, subsequent neurotracing experiments showed that crypt-like cells were also involved in detecting *Y. ruckeri*. Our results also showed fluorescent oval shaped cells within the epithelium after exposure to IHNV, which supports prior research (Sepahi et al., 2019). Crypt cells, which mediate antiviral immune responses, express Trk-A like receptors that directly detect IHNV; IHNV utilize this receptor as port of entry (Sepahi et al., 2019). Considering this, we suspect that detection of *Y. ruckeri* occurs in a similar fashion. However, the exact detection and entry mechanism *Y. ruckeri* is still to be described.

A comprehensive literature review has described the intestines, epithelial cells of the lateral line and the gills as potential portals of entry for *Y. ruckeri* (Guijarro et al., 2018; Ohtani, Villumsen, Koppang, & Raida, 2015). In particular, the intestines and gills are of interest due their classification as mucosa-associated lymphatic tissues (Guijarro et al., 2018). The gills, like the olfactory epithelium, make direct contact with the external environment. Therefore, it is possible that the entry mechanism of *Y. ruckeri* via the gills is similar in the OE. Specifically, the flagellum or O-antigens, found on *Yersinia* species, may play a role in bacterial attachment and entry into the host (Menanteau-Ledouble,

Lawrence, & El-Matbouli, 2018; Ohtani et al., 2015; Palumbo & Wang, 2006). Likewise, secretion of Yrp1 proteins, which have been used as an immunogen for vaccination against *Y. ruckeri* (Fernandez et al., 2003), might also be involved in the infectious process by interacting with formyl peptide receptors (FPRs) (Fernandez et al., 2003). FPRs are selectively expressed by vomeronasal sensory neurons (VSNR) and, in the immune system of rodents, have been shown to respond to N-formyl peptides (Liberles et al., 2009). FPRs are G-protein coupled receptors expressed in humans and mice; however, the exact role of FPRs is unknown (Yang & Chiu, 2017). In regards to aquatic species, FPRs have thus far only been detected in the Japanese grenadier anchovy (*Coilia nasus*) (Zhu, Wang, Tang, Wang, & Wang, 2017). Although the presence of FPRs have not been reported in trout, it is possible that FPR proteins, which are present in the OE of mammals and other fish, could potentially act as a portal of entry for *Y. ruckeri*.

Interestingly, research has also shown that microbes, their toxins and/or metabolites can activate neurons (nociceptors) that mediate pain and subsequently activate neural-immune circuits (Lagomarsino, Kostic, & Chiu, 2021). Thus, detection of bacterial antigens, toxins or metabolites might be an evolutionary conserved feature amongst vertebrates.

Our histological results also showed that exposure to *Y. ruckeri* not only activates cells to take up our fluorescent tracer in the peripheral organ, but to its transmission to the CNS. We localized fluorescence within the deepest layers of the optic tectum (OT) 14 days after intranasal vaccination, indicating the OT is a center of integration. The OT (superior colliculus in mammals) is vital for visuo-motor responses and consists of five neural regions from dorsal to ventral: stratum opticum (SO), stratum fibrosum et griseum

superficiale (SFGS), stratum griseum centrale (SGC) and the stratum album centrale and stratum griseum periventriculare (SAC/SPV) (Heap et al., 2018). As shown by our results, fluorescence was localized in the deeper regions of the optic tectum, specifically an area populated by sparse nuclei, such as the SGC or SAC/SPV. The SPV is known to receive projections from the dorsal hypothalamus in larval zebrafish, which is populated by dopaminergic neurons involved in motor behaviors (Heap et al., 2018). Furthermore, the deep layers of the OT integrate afferent and efferent inputs to elicit evasive and proactive motor movements (Suzuki, Pérez-Fernández, Wibble, Kardamakis, & Grillner, 2019). Although the OT integrates visual cues, it also receives neural outputs from the dorsomedial and ventrolateral regions of the telencephalon and the hypothalamus, both of which integrate olfactory impulses (Heap et al., 2018). In fact, olfactory mediated activation of the OT might be carried out via the olfacto-retinal centrifugal pathway, as described in zebrafish (Maaswinkel & Li, 2003). This pathway is comprised of terminal nerve cells (TN) within the OB that receives olfactory impulses. Axons of these TN cells project to the retina, where they synapse with dopaminergic interplexiform cells and retinal ganglion cells (RGCs) (Li et al., 2017). The latter cells then directly project to the hypothalamus, which is a center of behavioral modification (Harris & Carr, 2016). Thus, these projections, which derive from olfactory input, could potentially modulate the behavior noted in our results.

Our histology showed fluorescent stained cells in trout exposed to IHNV; however, we were unable to trace it to the OB and brain. Despite this, our results showed that olfactory exposure to IHNV modulated the secretion of neurosteroids. Overall, we saw a differential change in estradiol, androstenedione, testosterone, cortisol and sulfated

cortisol between the OB and brain, in the control and IHNV treated fish after 15 min of exposure. Our results showed a significant increase of estradiol within the OB and moderate decrease in estradiol within the brain in IHNV treated fishes. This transient increase of estradiol within the OB could be a preemptive measure to restrict infections within the OB before they reach the brain, by promoting anti-inflammatory response. Estradiol, which interacts with $E\alpha$ and $E\beta$ receptors, is synthesized by radial glial cells (RGCs) found in the OT (Scheld et al., 2020). Several studies have elucidated that estradiol is involved in regulating immune functions within the CNS.

Estradiol has demonstrated neuroprotective qualities, such as, dampening neuro-inflammation to reduce tissue damage, modulating activation of microglial cells and monocyte-derived macrophages, and neurogenesis (Scheld et al., 2020). This occurs when estradiol binds to estradiol receptors on microglia and macrophages, shifting them from a pro-inflammatory to an anti-inflammatory state, thereby preventing damage from prolonged inflammation (Bruce-Keller et al., 2000). Furthermore, the data demonstrated that estradiol is required for the expression of pro-inflammatory markers (IL-1, TLR2, TNF) by microglial cells in murine models that were treated with intracerebral LPS and viral infections (Soucy, Boivin, Labrie, & Rivest, 2005). Estradiol is notably recognized as an important factor in mitigating cell migration and synapse formation as well as regulating anti-apoptotic genes (Diotel et al., 2013; Pellegrini et al., 2016). Although this role of estradiol is most researched in mice, the expression of estrogen receptors has been documented in several regions of the goldfish (*Carassius auratus*) brain including the OB, hypothalamus and OT (Diotel et al., 2018). Similarly, estrogen receptors and aromatase B (an enzyme that converts androgens into estrogens) activity has been

documented in the brain of African cichlid fish (*Astatotilapia burtoni*), catfish and lungfish (Chaube & Mishra, 2012; Maruska & Fernald, 2010). Thus, the local synthesis of neural E2 may prove beneficial in mediating a rapid neural immune response to mitigate infection, and the role of estradiol, as described in mice, may provide a similar effect in the brain of teleost fish.

We also detected a decrease of androstenedione in the brain and an overall increase of testosterone in both the OB and brain tissues in IHNV treated samples. Androstenedione (AD), a derivative of DHEA, is an intermediate steroid that is converted to estrogens including estrone and estradiol or androgen testosterone (Gottfried-Blackmore, Sierra, Jellinck, McEwen, & Bulloch, 2008). Therefore, the decrease in AD could be due to its immediate conversion to testosterone, which reflects what was seen in our results. Testosterone's known immune role involves inducing expression of interleukins on mast cells in mice (Gubbels Bupp & Jorgensen, 2018). Lastly, we saw a slight increase of cortisol in the OB and brain and slight decrease in sulfated cortisol in the brain of IHNV treated samples. Cortisol is generally responsible for maintaining homeostasis in vertebrates and mitigating inflammation in the CNS (Dong, Zhi, Bhayana, & Wu, 2016).

To compare the olfacto-immunopathways of IHNV and *Y. ruckeri*, we measured neurosteroid concentrations in the OE, OB, and brain over the course of 15 minutes, 4 hours, 24 hours and 14 days. Our results also showed that intranasal delivery of *Y. ruckeri* did in fact modulate neurosteroid concentrations within all tissues. Within the OE, the concentration of control and treated samples were similar at 15 minutes and 14 days, but the overall cortisol concentration of samples was much lower after 4 hours and 24 hours.

Also, we detected a trend of cortisol levels decreasing after 15 minutes and increasing at 4 hours in the OE, OB, and brain of *Y. ruckeri* treated samples. After 24 hours, cortisol decreased in the OE and OB but increased in the brain. This decrease in cortisol within the OE, particularly after 15 minutes, could be attributed to cortisol's role in supporting the OE. Cortisol maintains the OE by inhibiting inflammatory cytokine production and reducing congestion and swelling (Chang & Glezer, 2018; Wang et al., 2017). In fact, delivery of exogenous cortisol has been used to alleviate olfactory dysfunction in human studies. (Chang & Glezer, 2018; Wang et al., 2017). It is also believed to be involved in OSN regeneration by inducing apoptosis of olfactory epithelial cells (Takanosawa, Nishino, Ohta, & Ichimura, 2009). Although the role of cortisol is well known to act by binding to glucocorticoid receptors in an organ, such as the brain, the expression of glucocorticoid receptors in the olfactory mucosa has not been extensively studied. Data has been primarily collected from murine models, and limited research has investigated the role of cortisol in the olfactory mucosa of teleosts. However, the concentration of cortisol analyzed in the OE and OB throughout the four groups was not precise. The standard error of control tissues for the 15 minute and 14-day groups in the OE, and the 24-hour group in the OB was high compared to the *Y. ruckeri* treated fish of the same groups; therefore, our results may not accurately represent our sample. The high variability could be attributed to the small amount of tissue from the sampled trout or our overall sample size. Despite this, our results suggest a trend in neurosteroid modulation that can be explored in future studies.

We also measured the concentration of estradiol after *Y. ruckeri* delivery. Our results showed that olfactory detection of *Y. ruckeri* increases estradiol in the OB after 15

minutes and 4 hours and significantly decreases estradiol in the brain after 15 minutes. Interestingly, these results paralleled our findings in IHNV treated fish in which estradiol increased in the OB but decreased in the brain. Although we did not measure the concentration of estradiol across various time periods, like with *Y. ruckeri*, this similarity suggests a commonality in the olfacto-immuno pathway of IHNV and *Y. ruckeri*. Considering this, the role of estradiol is expected to be the same as previously mentioned. These results support that, although detection of pathogens is mediated by different receptors, the integration of olfactory signals in brain elicits similar neurosteroid signals.

Lastly, we saw a decrease of progesterone 15 minutes post vaccination within the olfactory epithelium, but it then increased significantly ($p = .004$) after 4 hours. To our knowledge, characterization of progesterone and its effects within the olfactory tissue of fish or mammals has not been researched. Analysis of the bulb showed an overall decrease of progesterone at the same time points, but a subsequent increase within the brain at 4 hours. An increase of progesterone was also detected within the brain after 4 hours, but the overall concentration of this neurosteroid was very low (<20 pg of P per mg of brain). Beyond its reproductive effects, progesterone, like cortisol, has neuroprotective benefits. In mammals, research has shown that progesterone primarily mediates changes through its interaction with the progesterone receptors mPR and PGRMC1 (Meffre et al., 2013). The mPR is of particular interest due to its presence in the olfactory bulb of mice (Meffre et al., 2013). Research shows that progesterone's actions include modulating synaptogenesis and stimulating myelination. Furthermore, the extent of progesterone neuroprotective benefits has been demonstrated in both traumatic brain injury (TBI) and brain ischemia experimental models (Meffre et al., 2013). After

TBI, studies suggested that the progesterone-mPR interaction induces astrocytes and microglial cells in the damaged area, which then in turn release pro-inflammatory cytokines (Meffre et al., 2013). Although astrocytes aren't present in fish, astrocyte-like cells, known as astroglia, and microglial cells are present in the CNS of zebrafish (Jurisch-Yaksi, Yaksi, & Kizil, 2020; Lyons & Talbot, 2014; Scheib & Byrd-Jacobs, 2020). Thus, given the similarities of neurosteroid functions across vertebrates, it is likely that progesterone acts in a similar fashion in fish, but this has yet to be described.

Although the pool of literature on neurosteroids is large, their role remains elusive, particularly in fish. Further experiments need to be performed to clarify receptors and cells involved (in the periphery and CNS), their mechanism of action and their overall effects. Considering our results, we have demonstrated the presence of neurosteroids in the olfactory epithelium in fish. Additionally, we have shown that trout act as an excellent model for future studies.

Overall, research shows that neurosteroids play a multi-functional role in regulating the immune responses (Bruce-Keller et al., 2000; Murugan et al., 2019). However, besides influencing the immune response, we believe the differential changes in neurosteroid concentrations in the OB and brain induces an avoidant behavioral response when fish are exposed to pathogens. Pathogen and parasite avoidance has been observed in several species including worms, rodents and flies (Sarabian, Curtis, & McMullan, 2018). The nematode *Caenorhabditis elegans* has been shown to avoid pathogens such as *Pseudomonas aeruginosa* through conditioned exposure. More so, *C. elegans* are deterred from lawns contaminated with *Microbacterium nematophilum* as well as bacterial metabolites secreted by *Serratia marcescens* (Anderson & McMullan,

2018; Yang & Chiu, 2017). Avoidance behaviors have also been reported in rodents. A study showed that healthy mice did not spend a significant amount of time with Lipopolysaccharide endotoxin (LPS)-infected mice compared to the control. However, when pre-exposed to cadaverine (an odorant emitted from decaying tissue), mice spent significantly less time with LPS-infected mice compared to the control (Renault, Gheusi, & Aubert, 2008). In contrast to previously mentioned studies, the results from our behavioral trials were noted in unconditioned fish. Given the sensitivity of olfaction, our results suggest that rainbow trout can detect *Y. ruckeri* via olfaction and modulate their behavior to avoid it when *Y. ruckeri* is released as a cue. It is unlikely that the behavioral changes were due to other processes such as gustation (taste) or chemesthesis (activation of somatosensory nerves by chemical stimuli) because they require a higher concentration of tastants or chemical stimuli (Slack, 2016)

Neurosteroids are involved in mediating several behaviors including reproduction, socialization and aggression, but little is known on how they mediate avoidance (Patel, Choudhary, Chandra, Bhardwaj, & Tripathi, 2019). Progesterone and estradiol have been shown to influence avoidant and approaching behavior in rats (Kavaliers et al., 2021; Llana & Frye, 2009). Estradiol's effects on avoidance or fear driven behaviors are primarily focused on humans and rodents subjected to exogenous estradiol treatments and analysis of their behavior. One study saw that estradiol treated mice were more fearful and less active than vehicle (control) treated mice during open field tests (described as time spent in center of field) and dark-light transition tests (movement from dark to light compartments) (Morgan & Pfaff, 2001). Another study found that direct infusion of estradiol, to the anterior hypothalamus, rapidly (within 20 minutes) increased agonistic

behavior in hamsters (Heimovics et al., 2015). Similarly, exogenous administration of estrogen and progesterone decreases anxiety and increases approach-like behavior in the ovariectomized rats. (Llaneza & Frye, 2009). However, this data focuses on progesterone and estradiol produced within the gonads, but despite this, the role of these hormones is expected to similarly influence behavior when synthesized within the brain.

There is significantly less research on neurosteroids' effects on behavior in fish, but there is some evidence suggesting that systemic steroids alter behavior. For example, Crucian carp displaying fright reaction (form of avoidant behavior) had significantly higher plasma levels of circulating estradiol and testosterone, compared to crucian carp that were not (Lastein, Höglund, Mayer, Overli, & Døving, 2008). Similarly, another study found that increased cortisol levels were associated with behavioral avoidance in female sockeye salmon exposed to stressed conspecifics (Bett et al., 2016).

To further understand behavior modulation, research must be used to visualize neural pathway activity. Several methods have been used to investigate neural circuits and neural control of behavior including Ca^{2+} imaging, electrophysiology, and optogenetics (Issa et al., 2011). Despite this progress, there is limited literature that utilizes fluorescent tracing for visualization of olfactory neurocircuits as a research tactic. The interaction of an odorant with its respective receptor results in internalization of the receptor via endocytosis (Døving, Hansson, Backström, & Hamdani, 2011). When we intranasally delivered *Y. ruckeri* with Alexa fluor-conjugated dextran, the fluorescent dye was endocytosed and subsequently released from the vesicle to reveal a stained OSN. The transcytosis of dye to subsequent neurons, as we saw in the optic tectum, could be attributed to permeation of the dye through ion channels at the axonal and dendritic

region of neurons. In fact, it has been suggested that the dye FM1-43 enters sensory neurons through mechanotransduction channels through hair cells of the inner ear (Meyers et al., 2003). Thus, our findings demonstrate an efficient, but severely underutilized tool, to uncover olfactory neurocircuits.

Research focusing on the neurocircuits of aversive behavior in fish is also understudied. Current work primarily focuses on olfactory detection of alarm substances, released from predators, that trigger fear, anxiety, and aversive behaviors in goldfish and zebrafish (Hintz, Weihing, Bayer, Lonzarich, & Bryant, 2017). In fact, research shows that alarm substances activate crypt neurons, which then project to the dorsomedial glomeruli. Secondary neurons subsequently project to the telencephalon and hypothalamus, which as previously mentioned are areas of neurosteroid and behavior integration (Enjin & Suh, 2013; Roy, Ogawa, Maniam, & Parhar, 2021 Anderson, 2018 #239), thus, explaining a potential circuit that parallels our findings.

The olfactory system plays a key role in aquatic organisms' survival by detecting an array of odorants and subsequently modulating their behavior (Hoover, 2010). Olfactory mediated avoidance behavior could prove to be an advantageous survival mechanism by preventing or reducing potential infections caused by pathogens or pathogen-riddled substances, such as infected food or sick conspecifics. However, this is a novel area of research, and much is still unknown about the neural circuit in pathogen detection. Future work should focus on identifying other bacterial species that act similarly to *Y. ruckeri* and the receptors, cells, and regions of the brain involved in this olfactory process. By understanding this mechanism at the peripheral level, we can explore how this modulates physiological processes and subsequent behavioral responses.

Specifically, literature on neurosteroids and their multi-functional role in olfaction, immune regulation, and behavior modification has not been extensively studied in aquatic species. Therefore, substantial investigations are needed to understand these processes, and our results show that rainbow trout are suitable model organism for this line of work.

7. CONCLUSION

In conclusion, we believe that olfactory detection of *Y. ruckeri* and the subsequent behavioral response is due to neurosteroid production resulting from integration within the optic tectum. Although our results support our hypothesis, we failed to visualize fluorescence within the OB, which is the primary integration area of OSN axonic projections. Neural integration is a multi-tiered process comprised of primary, secondary, tertiary, or higher projections that are relayed upstream to induce changes within the brain. We believe that the OT is a tier in neural projections, but future studies should incorporate varying time stamps to visualize potential projections within the telencephalon or hypothalamus, or other regions of the brain. Furthermore, our results characterized the presence of neurosteroids within olfactory tissues of fish, and we demonstrated a correlation between neurosteroid concentrations and behavioral changes. Lastly, estradiol increased within the olfactory bulb in both IHNV and *Y. ruckeri* group analysis, implying commonality in olfactory integration of pathogens.

In summary, our findings demonstrate a connection in neural-endocrine-immune response that has not been previously described in fish and further support the notion that OSNs not only regulate immune response but also modulate neurosteroids.

REFERENCES

- Ahuja, G., Bozorg Nia, S., Zapilko, V., Shiriagin, V., Kowatschew, D., Oka, Y., & Korsching, S. I. (2014). Kappe neurons, a novel population of olfactory sensory neurons. *Scientific Reports*, *4*, 4037.
- Anderson, A., & McMullan, R. (2018). Neuronal and non-neuronal signals regulate *Caenorhabditis elegans* avoidance of contaminated food. *Philosophical transactions of the Royal Society of London. Series B, Biological sciences*, *373*(1751).
- Antunes, G., Sebastião, A. M., & Simoes de Souza, F. M. (2014). Mechanisms of regulation of olfactory transduction and adaptation in the olfactory cilium. *PLoS One*, *9*(8), e105531.
- Assefa, A., & Abunna, F. (2018). Maintenance of fish health in aquaculture: review of epidemiological approaches for prevention and control of infectious disease of fish. *Veterinary Medicine International*, *2018*.
- Bazaes, A., Olivares, J., & Schmachtenberg, O. (2013). Properties, projections, and tuning of teleost olfactory receptor neurons. *Journal of Chemical Ecology*, *39*(4), 451-464.
- Bazáes, A., & Schmachtenberg, O. (2012). Odorant tuning of olfactory crypt cells from juvenile and adult rainbow trout. *Journal of Experimental Biology*, *215*(10), 1740.
- Becerra, M., Manso, M. J., Rodriguez-Moldes, I., & Anadón, R. (1994). Primary olfactory fibres project to the ventral telencephalon and preoptic region in trout (*Salmo trutta*): a developmental immunocytochemical study. *Journal of Comparative Neurology*, *342*(1), 131-143.
- Bett, N. N., Hinch, S. G., & Yun, S.-S. (2016). Behavioural responses of Pacific salmon to chemical disturbance cues during the spawning migration. *Behavioural Processes*, *132*, 76-84.
- Bi, Z., Barna, M., Komatsu, T., & Reiss, C. S. (1995). Vesicular stomatitis virus infection of the central nervous system activates both innate and acquired immunity. *Journal of Virology*, *69*(10), 6466-6472.
- Biechl, D., Tietje, K., Gerlach, G., & Wullimann, M. F. (2016). Crypt cells are involved in kin recognition in larval zebrafish. *Scientific Reports*, *6*, 24590.
- Bremer, A. A., & Miller, W. L. (2014). Chapter 13 - regulation of steroidogenesis. In A. Ulloa-Aguirre & P. M. Conn (Eds.), *Cellular Endocrinology in Health and Disease* (pp. 207-227). Boston: Academic Press.

- Breyta, R., Brito, I., Ferguson, P., Kurath, G., Naish, K. A., Purcell, M. K., . . . LaDeau, S. (2017). Transmission routes maintaining a viral pathogen of steelhead trout within a complex multi-host assemblage. *Ecology and Evolution*, 7(20), 8187-8200.
- Bruce-Keller, A. J., Keeling, J. L., Keller, J. N., Huang, F. F., Camondola, S., & Mattson, M. P. (2000). Antiinflammatory effects of estrogen on microglial activation. *Endocrinology*, 141(10), 3646-3656. doi:10.1210/endo.141.10.7693
- Buck, L. (1996). Information coding in the vertebrate olfactory system. *Annual Review of Neuroscience*, 19, 517-544.
- Butowt, R., & Bilinska, K. (2020). SARS-CoV-2: olfaction, brain infection, and the urgent need for clinical samples allowing earlier virus detection. *ACS Chemical Neuroscience*, 11(9), 1200-1203.
- Carabotti, M., Scirocco, A., Maselli, M. A., & Severi, C. (2015). The gut-brain axis: interactions between enteric microbiota, central and enteric nervous systems. *Annals of gastroenterology*, 28(2), 203-209.
- Catania, S., Germanà, A., Laurà, R., Gonzalez, T., Ciriaco, E., & Vega, J. (2003). The crypt neurons in the olfactory epithelium of the adult zebrafish express TrkA-like immunoreactivity. *Neuroscience Letters*, 350, 5-8.
- Chang, S., & Glezer, I. (2018). The balance between efficient anti-inflammatory treatment and neuronal regeneration in the olfactory epithelium. *Neural Regeneration Research*, 13(10), 1711-1714.
- Chaube, R., & Mishra, S. (2012). Brain steroid contents in the catfish *Heteropneustes fossilis*: sex and gonad stage-specific changes. *Fish Physiology and Biochemistry*, 38(3), 757-767.
- Coumailleau, P., Pellegrini, E., Adrio, F., Diotel, N., Cano-Nicolau, J., Nasri, A., . . . Kah, O. (2015). Aromatase, estrogen receptors and brain development in fish and amphibians. *Biochimica et Biophysica Acta (BBA) - Gene Regulatory Mechanisms*, 1849(2), 152-162.
- Demb, J. B., & Singer, J. H. (2015). Functional Circuitry of the Retina. *Annu Rev Vis Sci*, 1, 263-289.
- Diotel, N., Charlier, T. D., Lefebvre d'Hellencourt, C., Couret, D., Trudeau, V. L., Nicolau, J. C., . . . Pellegrini, E. (2018). Steroid transport, local synthesis, and signaling within the brain: roles in neurogenesis, neuroprotection, and sexual behaviors. *Frontiers in Neuroscience*, 12(84).

- Diotel, N., Do Rego, J.-L., Anglade, I., Vaillant, C., Pellegrini, E., Vaudry, H., & Kah, O. (2011a). The brain of teleost fish, a source, and a target of sexual steroids. *Frontiers in Neuroscience*, *5*, 137-137.
- Diotel, N., Do Rego, J. L., Anglade, I., Vaillant, C., Pellegrini, E., Gueguen, M. M., . . . Kah, O. (2011b). Activity and expression of steroidogenic enzymes in the brain of adult zebrafish. *European Journal of Neuroscience*, *34*(1), 45-56.
- Diotel, N., Le Page, Y., Mouriec, K., Tong, S. K., Pellegrini, E., Vaillant, C., . . . Kah, O. (2010). Aromatase in the brain of teleost fish: expression, regulation and putative functions. *Frontiers in Neuroendocrinology*, *31*(2), 172-192.
- Diotel, N., Servili, A., Gueguen, M.-M., Mironov, S., Pellegrini, E., Vaillant, C., . . . Anglade, I. (2011c). Nuclear progesterone receptors are up-regulated by estrogens in neurons and radial glial progenitors in the brain of zebrafish. *PLoS One*, *6*(11), e28375.
- Diotel, N., Vaillant, C., Gabbero, C., Mironov, S., Fostier, A., Gueguen, M.-M., . . . Pellegrini, E. (2013). Effects of estradiol in adult neurogenesis and brain repair in zebrafish. *Hormones and Behavior*, *63*(2), 193-207.
- Do Rego, J. L., Seong, J. Y., Burel, D., Leprince, J., Vaudry, D., Luu-The, V., . . . Vaudry, H. (2012). Regulation of neurosteroid biosynthesis by neurotransmitters and neuropeptides. *Frontiers in Endocrinology*, *3*, 4-4.
- Døving, K., Hansson, K.-A., Backström, T., & Hamdani, E. (2011). Visualizing a set of olfactory sensory neurons responding to a bile salt. *Journal of Experimental Biology*, *214*, 80-87.
- Durrant, D. M., Ghosh, S., & Klein, R. S. (2016). The olfactory bulb: an immunosensory effector organ during neurotropic viral infections. *ACS Chemical Neuroscience*, *7*(4), 464-469.
- Enjin, A., & Suh, G. S.-B. (2013). Neural mechanisms of alarm pheromone signaling. *Molecules and cells*, *35*(3), 177-181.
- Fernandez, L., Lopez, J. R., Secades, P., Menendez, A., Marquez, I., & Guijarro, J. A. (2003). In Vitro and In Vivo Studies of the Yrp1 Protease from *Yersinia ruckeri* and Its Role in Protective Immunity against Enteric Red Mouth Disease of Salmonids. *Applied and Environmental Microbiology*, *69*(12), 7328. doi:10.1128/AEM.69.12.7328-7335.2003
- Gerlach, G., Tietje, K., Biechl, D., Namekawa, I., Schalm, G., & Sulmann, A. (2019). Behavioural and neuronal basis of olfactory imprinting and kin recognition in larval fish. *Journal of Experimental Biology*, *222*(Suppl 1), jeb189746.

- Gottfried-Blackmore, A., Sierra, A., Jellinck, P. H., McEwen, B. S., & Bulloch, K. (2008). Brain microglia express steroid-converting enzymes in the mouse. *The Journal of Steroid Biochemistry and Molecular Biology*, 109(1), 96-107.
- Gubbels Bupp, M. R., & Jorgensen, T. N. (2018). Androgen-Induced Immunosuppression. *Frontiers in Immunology*, 9(794).
- Guijarro, J. A., García-Torrico, A. I., Cascales, D., & Méndez, J. (2018). The infection process of yersinia ruckeri: reviewing the pieces of the jigsaw puzzle. *Frontiers in Cellular and Infection Microbiology*, 8, 218-218.
- Hamdani, E. H., & Døving, K. B. (2007). The functional organization of the fish olfactory system. *Progress in Neurobiology*, 82(2), 80-86.
- Hansen, A., & Zielinski, B. S. (2005). Diversity in the olfactory epithelium of bony fishes: development, lamellar arrangement, sensory neuron cell types and transduction components. *Journal of Neurocytology*, 34(3), 183-208.
- Hansson, K. A., Døving, K. B., & Skjeldal, F. M. (2015). Mixed input to olfactory glomeruli from two subsets of ciliated sensory neurons does not impede relay neuron specificity in the crucian carp. *Journal of Experimental Biology*, 218(Pt 20), 3257-3263.
- Harris, B. N., & Carr, J. A. (2016). The role of the hypothalamus-pituitary-adrenal/interrenal axis in mediating predator-avoidance trade-offs. *General and Comparative Endocrinology*, 230-231, 110-142.
- Heap, L. A., Vanwalleghem, G. C., Thompson, A. W., Favre-Bulle, I., Rubinsztein-Dunlop, H., & Scott, E. K. (2018). Hypothalamic Projections to the Optic Tectum in Larval Zebrafish. *Frontiers in Neuroanatomy*, 11(135).
- Heimovics, S. A., Trainor, B. C., & Soma, K. K. (2015). Rapid Effects of Estradiol on Aggression in Birds and Mice: The Fast and the Furious. *Integrative and Comparative Biology*, 55(2), 281-293.
- Hintz, H. A., Weihing, C., Bayer, R., Lonzarich, D., & Bryant, W. (2017). Cultured fish epithelial cells are a source of alarm substance. *MethodsX*, 4, 480-485.
- Hoover, K. C. (2010). Smell with inspiration: the evolutionary significance of olfaction. *American Journal of Physical Anthropology*, 143(S51), 63-74.
- Issa, F. A., Brien, G., Kettunen, P., Sagasti, A., Glanzman, D. L., & Papazian, D. M. (2011). Neural circuit activity in freely behaving zebrafish (&em>Danio rerio). *The Journal of Experimental Biology*, 214(6), 1028.

- Jurisch-Yaksi, N., Yaksi, E., & Kizil, C. (2020). Radial glia in the zebrafish brain: Functional, structural, and physiological comparison with the mammalian glia. *Glia*, 68(12), 2451-2470.
- Kasumyan, A. (2004). *The olfactory system in fish: structure, function, and role in behavior* (Vol. 44).
- Kavaliers, M., Bishnoi, I. R., Ossenkopp, K.-P., & Choleris, E. (2021). Differential effects of progesterone on social recognition and the avoidance of pathogen threat by female mice. *Hormones and Behavior*, 127, 104873.
- Kermen, F., Franco, L., Wyatt, C., & Yaksi, E. (2013). Neural circuits mediating olfactory-driven behavior in fish. *Frontiers in Neural Circuits*, 7(62).
- Lagomarsino, V. N., Kostic, A. D., & Chiu, I. M. (2021). Mechanisms of microbial–neuronal interactions in pain and nociception. *Neurobiology of Pain*, 9, 100056.
- LaPatra, S., Kao, S., Erhardt, E. B., & Salinas, I. (2015). Evaluation of dual nasal delivery of infectious hematopoietic necrosis virus and enteric red mouth vaccines in rainbow trout (*Oncorhynchus mykiss*). *Vaccine*, 33(6), 771-776.
- LaPatra, S. E., Lauda, K. A., Jones, G. R., Walker, S. C., Shewmaker, B. S., & Morton, A. W. (1995). Characterization of IHNV isolates associated with neurotropism. *Veterinary Research*, 26(5-6), 433-437.
- Lastein, S., Höglund, E., Mayer, I., Overli, O., & Døving, K. B. (2008). Female crucian carp, *Carassius carassius*, lose predator avoidance behavior when getting ready to mate. *Journal of Chemical Ecology*, 34(11), 1487-1491.
- Lerner, T. N., Ye, L., & Deisseroth, K. (2016). Communication in Neural Circuits: Tools, Opportunities, and Challenges. *Cell*, 164(6), 1136-1150.
- Li, L., Wojtowicz, J. L., Malin, J. H., Huang, T., Lee, E. B., & Chen, Z. (2017). GnRH-mediated olfactory and visual inputs promote mating-like behaviors in male zebrafish. *PLoS One*, 12(3), e0174143-e0174143.
- Liberles, S. D., Horowitz, L. F., Kuang, D., Contos, J. J., Wilson, K. L., Siltberg-Liberles, J., . . . Buck, L. B. (2009). Formyl peptide receptors are candidate chemosensory receptors in the vomeronasal organ. *Proceedings of the National Academy of Sciences*, 106(24), 9842.
- Llaneza, D. C., & Frye, C. A. (2009). Progestogens and estrogen influence impulsive burying and avoidant freezing behavior of naturally cycling and ovariectomized rats. *Pharmacology, biochemistry, and behavior*, 93(3), 337-342.

- Lyons, D. A., & Talbot, W. S. (2014). Glial cell development and function in zebrafish. *Cold Spring Harbor perspectives in biology*, 7(2), a020586-a020586.
- Maaswinkel, H., & Li, L. (2003). Olfactory input increases visual sensitivity in zebrafish: a possible function for the terminal nerve and dopaminergic interplexiform cells. *Journal of Experimental Biology*, 206(13), 2201.
- Maruska, K. P., & Fernald, R. D. (2010). Reproductive status regulates expression of sex steroid and GnRH receptors in the olfactory bulb. *Behavioural Brain Research*, 213(2), 208-217.
- Meffre, D., Labombarda, F., Delespierre, B., Chastre, A., De Nicola, A. F., Stein, D. G., . . . Guennoun, R. (2013). Distribution of membrane progesterone receptor alpha in the male mouse and rat brain and its regulation after traumatic brain injury. *Neuroscience*, 231, 111-124.
- Menanteau-Ledouble, S., Lawrence, M. L., & El-Matbouli, M. (2018). Invasion and replication of *Yersinia ruckeri* in fish cell cultures. *BMC Veterinary Research*, 14(1), 81.
- Meyers, J. R., MacDonald, R. B., Duggan, A., Lenzi, D., Standaert, D. G., Corwin, J. T., & Corey, D. P. (2003). Lighting up the Senses: FM1-43 Loading of Sensory Cells through Nonselective Ion Channels. *The Journal of Neuroscience*, 23(10), 4054.
- Miklavc, P., & Valentinčič, T. (2012). Chemotopy of amino acids on the olfactory bulb predicts olfactory discrimination capabilities of zebrafish (*Danio rerio*). *Chemical Senses*, 37(1), 65-75.
- Miwa, T., Moriizumi, T., Horikawa, I., Uramoto, N., Ishimaru, T., Nishimura, T., & Furukawa, M. (2002). Role of nerve growth factor in the olfactory system. *Microscopy Research and Technique*, 58(3), 197-203.
- Morgan, M. A., & Pfaff, D. W. (2001). Effects of estrogen on activity and fear-related behaviors in mice. *Hormones and Behavior*, 40(4), 472-482.
- Murugan, S., Jakka, P., Namani, S., Mujumdar, V., & Radhakrishnan, G. (2019). The neurosteroid pregnenolone promotes degradation of key proteins in the innate immune signaling to suppress inflammation. *Journal of Biological Chemistry*, 294(12), 4596-4607.
- Ohtani, M., Villumsen, K. R., Koppang, E. O., & Raida, M. K. (2015). Global 3D imaging of *Yersinia ruckeri* bacterin uptake in rainbow trout fry. *PLoS One*, 10(2), e0117263.
- Olivares, J., & Schmachtenberg, O. (2019). An update on anatomy and function of the teleost olfactory system. *PeerJ*, 7, e7808.

- Pägelow, D., Chhatbar, C., Beineke, A., Liu, X., Nerlich, A., van Vorst, K., . . . Fulde, M. (2018). The olfactory epithelium as a port of entry in neonatal neuroinfection. *Nature Communications*, *9*(1), 4269.
- Palumbo, R. N., & Wang, C. (2006). Bacterial invasion: structure, function, and implication for targeted oral gene delivery. *Curr Drug Deliv*, *3*(1), 47-53.
- Patel, S., Choudhary, M., Chandra, R. K., Bhardwaj, A. K., & Tripathi, M. K. (2019). Sex steroids exert a suppressive effect on innate and cell mediated immune responses in fresh water teleost, *Channa punctatus*. *Developmental & Comparative Immunology*, *100*, 103415.
- Payne, A. H., & Hales, D. B. (2004). Overview of steroidogenic enzymes in the pathway from cholesterol to active steroid hormones. *Endocrine Reviews*, *25*(6), 947-970.
- Peirs, C., & Seal, R. P. (2016). Neural circuits for pain: Recent advances and current views. *Science*, *354*(6312), 578-584.
- Pellegrini, E., Diotel, N., Vaillant-Capitaine, C., Perez Maria, R., Gueguen, M. M., Nasri, A., . . . Kah, O. (2016). Steroid modulation of neurogenesis: focus on radial glial cells in zebrafish. *Journal of Steroid Biochemistry and Molecular Biology*, *160*, 27-36.
- Renault, J., Gheusi, G., & Aubert, A. (2008). Changes in social exploration of a lipopolysaccharides-treated conspecific in mice: role of environmental cues. *Brain Behav Immun*, *22*(8), 1201-1207.
- Roy, N., Ogawa, S., Maniam, R., & Parhar, I. (2021). Habenula GPR139 is associated with fear learning in the zebrafish. *Scientific Reports*, *11*(1), 5549. doi:10.1038/s41598-021-85002-1
- Sarabian, C., Curtis, V., & McMullan, R. (2018). Evolution of pathogen and parasite avoidance behaviours. *Philosophical transactions of the Royal Society of London. Series B, Biological sciences*, *373*(1751), 20170256.
- Sato, K., & Suzuki, N. (2001). Whole-cell response characteristics of ciliated and microvillous olfactory receptor neurons to amino acids, pheromone candidates and urine in rainbow trout. *Chemical Senses*, *26*(9), 1145-1156.
- Scheib, J., & Byrd-Jacobs, C. (2020). Zebrafish Astroglial Morphology in the Olfactory Bulb Is Altered With Repetitive Peripheral Damage. *Frontiers in Neuroanatomy*, *14*, 4.

- Scheld, M., Heymann, F., Zhao, W., Tohidnezhad, M., Clarner, T., Beyer, C., & Zendedel, A. (2020). Modulatory effect of 17 β -estradiol on myeloid cell infiltration into the male rat brain after ischemic stroke. *The Journal of Steroid Biochemistry and Molecular Biology*, 202, 105667.
- Sepahi, A., Kraus, A., Casadei, E., Johnston, C. A., Galindo-Villegas, J., Kelly, C., . . . Salinas, I. (2019). Olfactory sensory neurons mediate ultrarapid antiviral immune responses in a TrkA-dependent manner. *Proceedings of the National Academy of Sciences*, 116(25), 12428-12436.
- Sepahi, A., Kraus, A., Galindo-Villegas, J., Kelly, C., Garcia-Moreno, D., Mulero, V., . . . Salinas, I. (2018). The immunological role of crypt olfactory neurons against neurotropic viruses in teleost fish. *Journal of Immunology*, 200 (1 Supplement), 173.115-173.115.
- Siddiqui, A. N., Siddiqui, N., Khan, R. A., Kalam, A., Jabir, N. R., Kamal, M. A., . . . Tabrez, S. (2016). Neuroprotective role of steroidal sex hormones: an overview. *CNS Neuroscience* 22(5), 342-350.
- Slack, J. P. (2016). Chapter 21 - Molecular Pharmacology of Chemesthesis. In F. Zufall & S. D. Munger (Eds.), *Chemosensory Transduction* (pp. 375-391): Academic Press.
- Soucy, G., Boivin, G., Labrie, F., & Rivest, S. (2005). Estradiol is required for a proper immune response to bacterial and viral pathogens in the female brain. *Journal of Immunology*, 174(10), 6391-6398.
- Sunshine, M. D., Sutor, T. W., Fox, E. J., & Fuller, D. D. (2020). Targeted activation of spinal respiratory neural circuits. *Experimental Neurology*, 328, 113256.
- Suzuki, D. G., Pérez-Fernández, J., Wibble, T., Kardamakias, A. A., & Grillner, S. (2019). The role of the optic tectum for visually evoked orienting and evasive movements. *Proceedings of the National Academy of Sciences*, 116(30), 15272.
- Takanosawa, M., Nishino, H., Ohta, Y., & Ichimura, K. (2009). Glucocorticoids enhance regeneration of murine olfactory epithelium. *Acta Oto-Laryngologica*, 129(9), 1002-1009.
- Verburg-van Kemenade, B. M. L., Stolte, H. H., Metz, J., & Chadzinska, M. (2009). Neuroendocrine-immune interactions in teleost fish. *Fish Neuroendocrinology*, 28.
- Vielma, A., Ardiles, A., Delgado, L., & Schmachtenberg, O. (2008). The elusive crypt olfactory receptor neuron: evidence for its stimulation by amino acids and cAMP pathway agonists. *Journal of Experimental Biology*, 211(15), 2417-2422.

- Wang, X., Zhu, Y., Ni, D., Lv, W., Gao, Z., & Qi, F. (2017). Intranasal application of glucocorticoid alleviates olfactory dysfunction in mice with allergic rhinitis. *Experimental and therapeutic medicine*, *14*(5), 3971-3978.
- Wetzel, C. H., Brunert, D., & Hatt, H. (2005). Cellular mechanisms of olfactory signal transduction. *Chemical Senses*, *30*(suppl_1), i321-i322.
- Wrobel, A., Leo, J. C., & Linke, D. (2019). Overcoming Fish Defences: The Virulence Factors of *Yersinia ruckeri*. *Genes*, *10*(9), 700.
- Yang, N. J., & Chiu, I. M. (2017). Bacterial signaling to the nervous system through toxins and metabolites. *Journal of Molecular Biology*, *429*(5), 587-605.
- Yong, C. Y., Ong, H. K., Tang, H. C., Yeap, S. K., Omar, A. R., Ho, K. L., & Tan, W. S. (2019). Infectious hematopoietic necrosis virus: advances in diagnosis and vaccine development. *PeerJ*, *7*, e7151-e7151.
- Zhu, G., Wang, L., Tang, W., Wang, X., & Wang, C. (2017). Identification of olfactory receptor genes in the Japanese grenadier anchovy *Coilia nasus*. *Genes Genomics*, *39*(5), 521-532.